Bull Volcanol (1996) 58:205–225



ORIGINAL PAPER



Th. Thordarson · S. Self · N. Óskarsson
T. Hulsebosch

# Sulfur, chlorine, and fluorine degassing and atmospheric loading by the 1783–1784 AD Laki (Skaftár Fires) eruption in Iceland

Received: 30 May 1995 / Accepted: 19 April 1996

**Abstract** The 1783–1784 Laki tholeiitic basalt fissure eruption in Iceland was one of the greatest atmospheric pollution events of the past 250 years, with widespread effects in the northern hemisphere. The degassing history and volatile budget of this event are determined by measurements of pre-eruption and residual contents of sulfur, chlorine, and fluorine in the products of all phases of the eruption. In fissure eruptions such as Laki, degassing occurs in two stages: by explosive activity or lava fountaining at the vents, and from the lava as it flows away from the vents. Using the measured sulfur concentrations in glass inclusions in phenocrysts and in groundmass glasses of quenched eruption products, we calculate that the total accumulative atmospheric mass loading of sulfur dioxide was 122 Mt over a period of 8 months. This volatile release is sufficient to have generated ~250 Mt of $H_2SO_4$ aerosols, an amount which agrees with an independent estimate of the Laki aerosol yield based on atmospheric turbidity measurements. Most of this volatile mass (~60 wt.%) was released during the first 1.5 months of activity. The measured chlorine and fluorine concentrations in the samples indicate that the atmospheric loading of hydrochloric acid and hydrofluoric acid was ~7.0 and 15.0 Mt, respectively. Furthermore, ~75% of the volatile mass dissolved by the Laki magma was released at the vents and carried by eruption columns to altitudes between 6 and 13 km. The high degree of degassing at the vents is attributed to development of a separated two-phase flow in the upper magma conduit, and implies that high-discharge basaltic eruptions such as Laki are able to loft huge quantities of gas to altitudes where the resulting aerosols can reside for months or even 1–2 years. The atmospheric volatile contribution due to subsequent degassing of the Laki lava flow is only 18 wt.% of the total dissolved in the magma, and these emissions were confined to the lowest regions of the troposphere and therefore important only over Iceland. This study indicates that determination of the amount of sulfur degassed from the Laki magma batch by measurements of sulfur in the volcanic products (the petrologic method) yields a result which is sufficient to account for the mass of aerosols estimated by other methods.

**Key words** Laki · Effusive basaltic volcanism · Fissure eruption · Eruption dynamics · Magma degassing · Volcanic gases · Volcanic glass chemistry · Volcanic aerosols

Editorial responsibility: J. McPhie

Th. Thordarson (✉)[1] · S. Self · T. Hulsebosch
Department of Geology and Geophysics, School of Ocean and Earth Sciences and Technology, University of Hawaii at Manoa, Honolulu, Hawaii 96822, USA
Fax: +64 737 48199
e-mail: t.thordarson@gns.cri.nz

N. Óskarsson
Nordic Volcanological Institute, University of Iceland, 101 Reykjavík, Iceland

*Present address:*
[1]Wairakei Research Centre, Institute of Geological and Nuclear Sciences Limited, State Highway 1, Wairakei, Private Bag 2000, Taupo, New Zealand

## Introduction

The growing interest over the past 20 years in the effects of volcanic eruptions on global climate has concentrated almost exclusively on large silicic explosive eruptions such as Tambora 1815, Krakatau 1883, and Pinatubo 1991 (e.g., Self et al. 1981; McCormick et al. 1995). However, large basaltic lava-producing eruptions, such as the Laki (Skaftár Fires) event in Iceland, 64°10′N, 17°15′W, in 1783–1784, are also known to have been linked to locally cooler weather and unusual atmospheric phenomena (Thorarinsson 1979, 1981; Sigurdsson 1982; Angell and Korshover 1985; Wood 1992; Stothers 1996; Thordarson 1995). Such eruptions have the potential to release great amounts of gas into the atmosphere, but studies have not been carried out on the details of the volatile emissions in terms of effi-

ciency of magma degassing, mechanisms and rates during eruption, heights of atmospheric volatile release, and accurate estimates of the masses of volatile species released.

Previous estimates of the amount of $SO_2$ released by the Laki eruption (Sigurdsson 1982; Óskarsson et al. 1984; Devine et al. 1984) range from 56 to 63 Mt when corrected for the new volume estimates for the Laki eruption products (Thordarson and Self 1993). Metrich et al. (1991) showed that three glass inclusions of Laki composition trapped in phenocrysts within phreatomagmatic clasts of the Laki tephra contained on average $1810 \pm 100$ ppm of sulfur, a considerably higher amount than the values of 800–960 ppm S used by Sigurdsson (1982), Óskarsson et al. (1984), and Devine et al. (1984). Although the phreatomagmatic tephra constitutes only approximately 0.5% of the total amount of magma erupted, the analyses of Metrich et al. (1991) are in good agreement with the results presented in this study (see below).

In this paper we address the degassing history and the volatile budget of the Laki eruption as revealed by the concentrations of S, Cl, and F in the products of all phases of the eruption. We present new major element and volatile analyses of 17 glass inclusions from Laki phenocrysts and of groundmass glass in quenched products. These data establish new and more accurate estimates of the atmospheric mass loading of gases by Laki and show that the volatile release by the eruption was considerably greater than has been estimated previously. The new fluorine and chlorine data indicate that Laki released large quantities of HF and HCl into the atmosphere, a previously unquantified, but not unexpected, occurrence during the Laki eruption (Thorarinsson 1979, 1981). We also evaluate how degassing processes relate to the eruption mechanism and the rate of magma degassing during eruption.

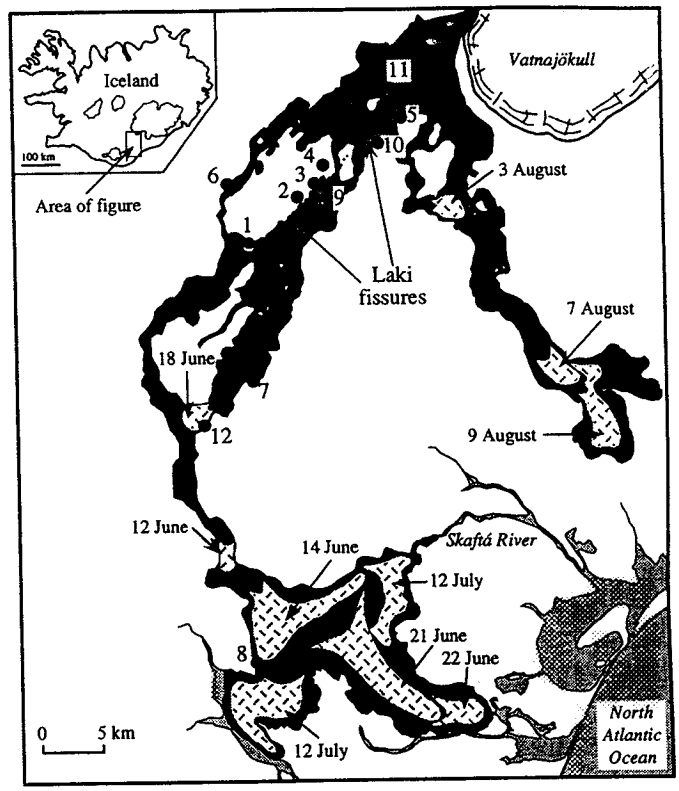


**Fig. 1** Map of the Laki fissures and lava flow field, Iceland, showing locations (numbered 1–12) where the samples used in this study were collected (see text for discussion). *Stippled areas* denote locations of flow fronts on date shown and are reconstructed according to descriptions given by Reverend Jón Steingrímsson (1783, 1788)

## The 1783–1784 Laki eruption

### Nature of the eruption

The Laki fissure eruption lasted for 8 months, from 8 June 1783 to 7 February 1784, and produced one of the largest recorded basaltic lava flows, $14.7 \pm 1$ km$^3$ (Fig. 1). In addition, it produced 0.4 km$^3$ (dense rock equivalent) of tephra, giving the total volume of 15.1 km$^3$ used in this paper. Over 60% of the volume was erupted during the first 1.5 months of activity, and 90% by the end of the fifth month (Fig. 2). Ten eruption episodes occurred during the first 5 months of activity. Each began with a seismic swarm of increasing intensity and formation of a new fissure segment, followed by a short-lived explosive phase leading into lava

**Fig. 2** Illustration of sequence of events during the Laki eruption up to eruption episode X. Eruption episodes are shown in *row 1*, labeled I–X; S, strombolian fall units; P, phreatomagmatic fall units. *Row 2* shows the primary fall units produced by the eruption episodes. *Row 3* designates earthquake swarms; the *horizontal bars* show the duration of each swarm. Timing of explosive activity is shown in *row 4*, where *eruption clouds* denote explosive activity at Laki fissures. Row 5 (*stippled area*) shows qualitatively the fluctuations in lava production during the eruption; *h* and *l* indicate high and low discharge, respectively (not to scale). *Vertical arrows* mark the beginning and end of Laki fissure eruption and the *60%* and *90%* refer to volume fraction erupted up to that time. (Modified from Thordarson and Self 1993)

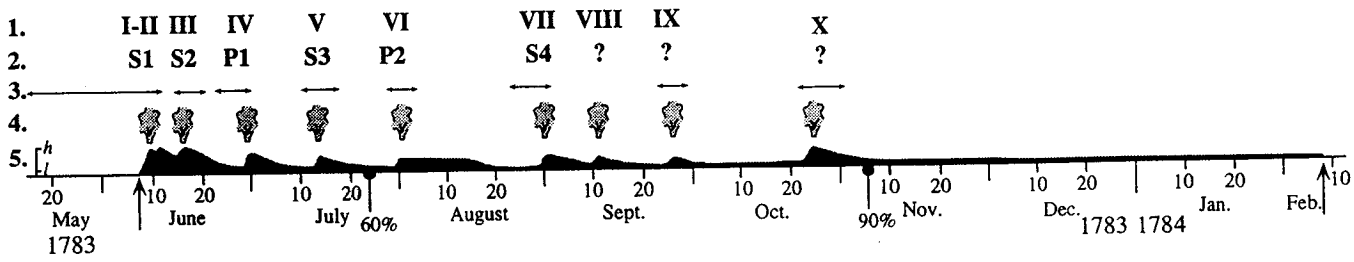

**Table 1** Laki sample locations and sample descriptions

| Sample location | Label | Description | Unit[a] |
|---|---|---|---|
| **Vent tephra** | | | |
| Location 1; Hnúta, section 133[b] | LS1-01 | Strombolian scoria lapilli | S1 |
| Location 12, Leidólfsfell | LS1-04 | Strombolian ash | S1 |
| Location 2, Vikradalur, section 94[b] | LS2-06 | Strombolian scoria lapilli | S2 |
| Location 3, Hverfjall, section TC-1 | LP1-U2 | Phreatomagmatic tephra | P1 |
| | LP1-U3 | Phreatomagmatic tephra | P1 |
| | LP1-U5 | Phreatomagmatic tephra | P1 |
| Location 4, Lambavatn, section 153[b] | LS3-02 | Strombolian scoria lapilli, base of unit | S3 |
| | LS3-03 | Strombolian scoria lapilli, top of unit | S3 |
| Location 5, Innrieyrar, section 75[b] | LP2-05 | Phreatomagmatic tephra | P2 |
| | LS4-01 | Strombolian scoria lapilli | S4 |
| **Lava flow** | | | |
| Location 6, Kambar | L-20 | Surface lava selvage | E1-FU4 |
| | L-21 | Basal lava selvage | E2-FU4 |
| Location 7, Kálfá | L-23 | Basal lava selvage | KAFU |
| Location 12, Leidólfsfell | LEI-04 | Lava core | LEIFU |
| | LEI-12 | Lava crust | LEIFU |
| Location 8, Eldvatnsbrú | L-24 | Basal lava selvage | SAL-9 |
| | L-25 | Surface lava selvage | SAL-9 |
| **Rootless cone tephra** | | | |
| Location 9, Varmárdalur | VRC-9 | Scoria lapilli | VRCTE |
| | VRC-11 | Scoria lapilli | VRCTE |
| Location 10, Blængur | BRC-9 | Scoria lapilli | BRCTE |
| Location 11, North of Innrieyrar | NIRC-7 | Scoria lapilli | NIRCTE |
| Location 12, Leidólfsfell | LEIRC-03 | Scoria lapilli | LEIRCU2 |
| | LEIRC-03A | Scoria lapilli | LEIRCU2 |
| | LEIRC-04 | Ash | LEIRCU1 |
| | LEIRC-12 | Scoria lapilli | LEIRCU2 |
| | LEIRC-20A | Ash | LEIRCU1 |

[a] Primary tephra fall units are designated as in Thordarson and Self (1993); S and P denote strombolian and phreatomagmatic fall units, respectively. Lava flow units are described in Appendix I. Unit designation for rootless cone tephra are based on unpublished tephra sections measured by Th. Thordarson

[b] Section designation from Thordarson (1990)

fountaining and effusive activity characterized by voluminous lava surges. The magma volume erupted by each episode ranged from ~0.5–2.0 $km^3$ and the volume ratio of tephra to lava was ~1/35. Magma discharge varied considerably during the eruption with highest eruption rates in the range of $2–5 \times 10^3\ m^3\ s^{-1}$ occurring during each eruptive episode (Fig. 2). During the first 5 months of activity, the mean discharge was of the order of $1–2.5 \times 10^3\ m^3\ s^{-1}$. The episodic nature of the eruption cannot be attributed to separate inflation–deflation events within the Laki reservoir because of the high magma fluxes and the short time which elapsed between successive episodes. Evaluation of the timing and sequence of events suggest that unsteady or non-uniform conduit flow was responsible for the episodic behavior of the eruption (Thordarson and Self 1993).

Each explosive phase lasted for hours to a few days and was characterized by either magmatic or hydromagmatic activity, producing a tephra deposit which consists of at least six mappable strombolian and phreatomagmatic fall units. The strombolian fall units (S1–S4; Table 1) account for ~80% of the total tephra volume, whereas the phreatomagmatic fall units (P1 and P2; Table 1) make up the remaining ~20%. The Laki fire fountains extended to heights of 800–1450 m during periods of peak magma discharge (Thordarson 1990). Historic evidence and calculations indicate that the Laki eruption column reached maximum altitudes of 11–13 km at times of vigorous activity, and that the eruption maintained 7- to 9-km-high columns during the first 5 months (Thordarson and Self 1993; Woods 1993). The tropopause over this region is at 9-10 km. As is demonstrated below, vent degassing, especially during periods of vigorous explosive activity and fountaining, is responsible for release of the bulk (~80%) of the volatiles during the Laki eruption, whereas degassing of lava during transport and cooling accounts for the remaining 20%.

## Whole-rock compositions

The Laki products are glomeroporphyritic quartz-tholeiite basalt containing ~5.5 vol.% of euhedral phenocrysts ranging in size from 0.2 to 3.0 mm. The glomerocrysts contain one, two, or more rarely, all of the following crystal phases: plagioclase ($An_{90–55}$), olivine ($Fo_{86–68}$) and clinopyroxene ($Wo_{40}En_{45}Fs_{14.5}$), and are in compositional equilibrium with the erupted magma (Grönvold 1984; Metrich et al. 1991). Laki tephra and lava (Fig. 3) show a small spatial and temporal compositional variance in major element concentrations (Bell and Humphries 1972; Grönvold 1984). Uniform U and

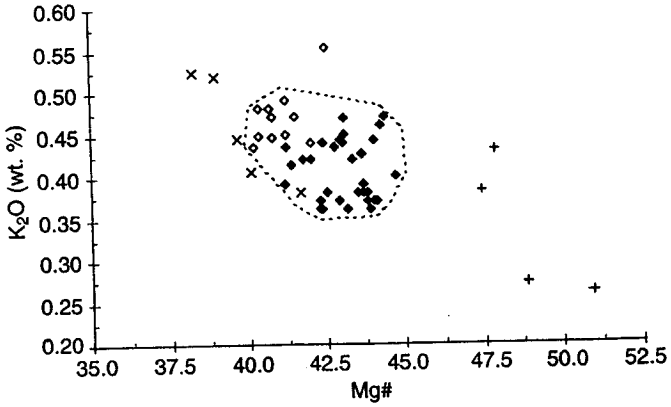


**Fig. 3** Compositional variations of eruption products within the Grímsvötn volcanic system (GVS). $K_2O$ (wt.%) variation as a function of Mg# (calculated as [Mg/(Mg+Fe)]×100). Laki samples are indicated by *open* (tephra) and *filled* (lava) *diamonds*. *Plusses* represent other subaerial lavas within the GVS and *crosses* denote tephra samples from the subglacial Grímsvötn central volcano. *Broken line* outlines the field defined by the Laki eruption products. Major element data are from this study and the sources given in Thordarson (1995)

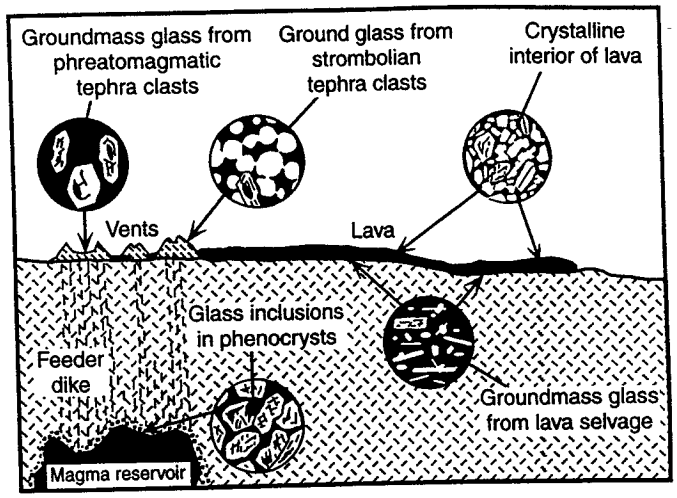


**Fig. 4** Illustration (not to scale) of the Laki eruption viewed from the southwest showing the type of samples (*arrows*) collected for this study. *Glass inclusions in phenocrysts* represent the undegassed magma fraction residing in a reservoir at depth prior to eruption. *Groundmass glass from phreatomagmatic tephra clasts* represents partly degassed magma which froze in the feeder dike due to interaction with external water. *Groundmass glass of strombolian tephra clasts* represents magma which degassed at the vents. Lava selvages characterize magma which has gone through the stage of vent degassing and, in addition, has liberated a fraction of its remaining volatiles as the lava flowed away from the fissures. Crystalline lava denotes magma which has gone through the stages of vent and lava emplacement degassing and has lost an additional fraction of its volatiles during cooling and crystallization. It also contains the volatiles which did not escape from the lava into the atmosphere

Th abundances (0.344±0.007 ppm and 1.12±0.02 ppm, respectively) demonstrate the homogeneity of the Laki magma; differences in measured concentrations in samples from all main eruptive units are <7% (Sigmarsson et al. 1991). The apparent uniformity of the Laki magma is remarkable in view of the duration of the eruption and the large volume of magma involved.

## Sample collection and analytical methods

### Samples and their significance

Samples representing the main phases of the Laki eruption were collected at 12 different locations within the lava flow and along the fissures (Fig. 1; Table 1). The types of samples collected for analyses are shown schematically in Fig. 4.

Tephra samples, representing mappable fall units, were collected at locations 1–5. A complete proximal section through the Laki flow is not available within 10 km from source, whereas in the medial (10–30 km from source) and distal (>30 km from source) areas the best outcrops occur in river channels (Fig. 1). Locations 6, 7, 8, and 12 represent measured sections through the Laki lava flow where samples of the lava interior and basal glass selvage were collected (Fig. 4; Table 1). Samples were also collected from the rootless cone groups at locations 9, 10, 11, and 12. These samples together represent flow units emplaced in June and July 1783 (locations 7, 8, 9, and 12), and from August through October 1783 (locations 6, 10, and 11). The significance of the samples is discussed further in Appendix I.

### Analytical procedure

Modes and vesicularity of representative tephra and lava samples were estimated by point counting of ~1000 points per thin section. Microprobe analyses used instrumental settings of 15 kV for the accelerating voltage, 15–20 nA in a beam-current-regulated mode, and a 5–20 μm focused beam in major element analyses of glass. Precision ($2\sigma$) for major elements is better than 1%. Analyses of S and Cl were conducted by the Cameca Trace routine, using the same general setup and counting time of 200 s. Based on counting statistics the precision for sulfur is 80 ppm and for Cl it is 60 ppm at the $2\sigma$ level. The same samples were also analyzed for S, Cl, and F by using the CSIRO-trace routine of Robinson and Graham (1992) with 15 kV accelerating voltage, 80 nA beam current, 10 μm focused beam, and counting time of 400 s. Precision ($2\sigma$) for S=35 ppm, Cl=30 ppm, and F=90 ppm. Raw data were corrected using the standard ZAF procedures. The Juan de Fuca glass standard VG2 and Makoupuhi glass standard A99 were analyzed as unknowns for S, Cl, and F during each analytical session and, as shown in Table 2a, our S values for both standards are in good agreement with Dixon et al. (1991). Precision and accuracy of the Cl and F microprobe analyses was tested by analyzing the MORB glass samples TR 154 21D-3 and TR 138 6D-1

**Table 2a** Representative microprobe analyses of international standards by Cameca and CSIRO trace routines

| | VG-2 | S | Cl | F | *N* | A-99 | S | Cl | F | *N* |
|---|---|---|---|---|---|---|---|---|---|---|
| | Reported | 1340[a] | n.a. | n.a. | 19 | | 170[a] | n.a. | n.a. | 15 |
| | SD | 80 | – | – | | | 30 | – | – | |
| Cameca trace routine | This study | 1348 | 291 | n.a. | 134 | | 135 | 229 | n.a. | 37 |
| | SD | 62 | 52 | – | | | 50 | 49 | – | |
| CSIRO trace routine | This study[b] | 1365 | 316 | 300 | 139 | | 220 | 227 | 765 | 42 |
| | SD | 29 | 19 | 72 | | | 12 | 20 | 79 | |

SD, standard deviation; n.a., not analysed; *N*, number of analyses
[a] Value reported by Dixon et al. (1991)
[b] Represents an average of analyses conducted over a period of 2 years by Th. Thordarson, S. B. Sherman, and L. Norby

**Table 2b** New CSIRO trace routine analyses of basalt glass samples from Michael and Schilling (1989)

| | TR 154 21D-3 | S | Cl | F | *N* | TR 138 6D-1 | S | Cl | F | *N* |
|---|---|---|---|---|---|---|---|---|---|---|
| | Reported | n.a. | 404[a] | 520[a] | | | n.a. | 44[a] | 280[a] | |
| CSIRO trace routine | This study[b] | 977 | 488 | 546 | 11 | | 1050 | 48 | 282 | 19 |
| | SD | 26 | 31 | 65 | | | 24 | 12 | 82 | |

SD, standard deviation; n.a., not analysed; *N*, number of analyses
[a] Values reported by Michael and Schilling (1989)
[b] Analyst: L. Norby

from Michael and Schilling (1989), and our results are compatible with theirs (Table 2b).

The $H_2O$ and $CO_2$ values used in this paper are from Óskarsson et al. (1984), which were obtained by Quadropol mass spectrometry on gasses released by vacuum fusion of crystalline lava, fibrous tephra, and crushed plagioclase phenocrysts rich in glass inclusions. The measured $CO_2$ values for glass inclusions may overestimate the concentration initially dissolved in the Laki magma, because it is likely that small $CO_2$ bubbles were present as a free volatile phase in Laki phenocrysts (Metrich et al. 1991). The method may also overestimate the $CO_2$ concentration dissolved in the groundmass glass of tephra, because the fibrous tephra clasts contain rare liquid-filled microbubbles (Ólafsson et al. 1984). Despite these uncertainties, we chose to use the $CO_2$ values of Óskarsson et al. (1984), because it is the only comprehensive data set which includes measurements of $CO_2$ inclusions, tephra, and crystalline lava.

**Fig. 5** Transmitted-light photomicrograph of a 60-×25-μm light-brown glass inclusion in plagioclase (sample L-21). The *dark circular spot* in the lower right corner is a bubble. *Scale bar* is 100 μm

## Petrology and glass chemistry

In this section we outline the major element and volatile chemistry of glass inclusions and groundmass glass in quenched products of the Laki eruption. The chemistry of single samples is listed in Appendix II.

### Glass inclusion

All of the Laki phenocryst phases contain clear, light-brown glass inclusions and sparse inclusions of dark-brown, transparent glass, ranging from ≤1 to 500 μm in the longest dimensions (Fig. 5). Common inclusions are between 20 and 120 μm in size and of spherical or oblate shape (Thordarson 1995). Some inclusions contain vapor bubbles.

Major element microprobe analyses of more than 30 glass inclusions from Laki phenocrysts were performed to locate inclusions of composition similar to the bulk Laki magma. Several inclusions showed clear evidence of extensive postentrapment host crystallization (Table 3) and were therefore not considered further. Measured major element concentrations of inclusions L-i-7, L-i-8, and L-i-11 trapped in olivine phenocrysts (Table A-1, Appendix II), demonstrate that the glass composition has been slightly affected by host crystalliza-

**Table 3** Major and volatile element composition of Laki glass inclusions

| | $SiO_2$ | $TiO_2$ | $Al_2O_3$ | FeO | MnO | MgO | CaO | $Na_2O$ | $K_2O$ | $P_2O_5$ | Sum | S | Cl | F | Mg# | *N* |
|---|---|---|---|---|---|---|---|---|---|---|---|---|---|---|---|---|
| Group 1 | 49.68 | 2.96 | 13.05 | 13.78 | 0.22 | 5.78 | 10.45 | 2.84 | 0.42 | 0.28 | 99.45 | 1677 | 310 | 665 | 42.77 | 21/23 |
| SD | 0.36 | 0.17 | 0.48 | 0.61 | 0.03 | 0.30 | 0.28 | 0.12 | 0.05 | 0.05 | 0.34 | 225 | 59 | 101 | | |
| Group 2 | 49.27 | 3.03 | 12.08 | 15.33 | 0.23 | 5.96 | 10.41 | 2.43 | 0.48 | 0.31 | 99.77 | 1632 | 246 | 537 | 40.92 | 6/6 |
| SD | 0.70 | 0.06 | 0.37 | 0.59 | 0.01 | 0.44 | 0.18 | 0.03 | 0.09 | 0.04 | 0.15 | 171 | 56 | 90 | | |
| Group 3 | 48.87 | 3.43 | 13.08 | 16.31 | 0.22 | 4.70 | 9.56 | 2.57 | 0.45 | 0.35 | 99.77 | 1622 | 298 | 660 | 33.92 | 6/6 |
| SD | 0.01 | 0.04 | 0.11 | 0.07 | 0.04 | 0.11 | 0.08 | 0.02 | 0.04 | 0.03 | 0.37 | 493 | 18 | 71 | | |
| Group 4 | 49.13 | 2.00 | 12.03 | 13.41 | 0.23 | 8.47 | 11.37 | 2.47 | 0.39 | 0.17 | 99.67 | 1675 | 198 | 562 | 50.44 | 4/5 |
| SD | 0.04 | 0.02 | 0.01 | 0.11 | 0.03 | 0.14 | 0.02 | 0.05 | 0.01 | 0.01 | 0.06 | 50 | 45 | 70 | | |
| Unaffected by host crystallization | | | | | | | | | | | | | | | | |
| L-i-3 | 49.61 | 2.85 | 13.07 | 13.88 | 0.24 | 5.77 | 10.39 | 3.01 | 0.42 | 0.25 | 99.50 | 1520 | 300 | 705 | 42.56 | 5 |
| SD | 0.16 | 0.03 | 0.07 | 0.15 | 0.03 | 0.15 | 0.09 | 0.05 | 0.02 | 0.04 | 0.40 | 25 | 55 | 10 | | |
| Affected by host crystallization[a] | | | | | | | | | | | | | | | | |
| L-i-18 | 48.42 | 2.67 | 7.37 | 16.48 | 0.22 | 10.44 | 11.30 | 1.80 | 0.31 | 0.23 | 99.25 | 1555 | 260 | 460 | 53.03 | 2 |
| SD | 0.01 | 0.12 | 0.63 | 0.08 | 0.04 | 0.30 | 0.08 | 0.30 | 0.07 | 0.01 | 0.65 | 90 | 85 | 130 | | |
| Laki whole-rock composition | | | | | | | | | | | | | | | | |
| L-lava | 49.63 | 2.68 | 13.87 | 13.45 | 0.22 | 5.73 | 10.40 | 2.69 | 0.41 | 0.33 | 99.28 | | | | 43.13 | 32 |
| SD | 0.62 | 0.13 | 0.31 | 0.34 | 0.01 | 0.22 | 0.20 | 0.15 | 0.04 | 0.06 | 1.03 | | | | 0.97 | |

Mg# = 100 Mg/(Mg + Fe*), Fe* = total Fe; *N*, number of analyses – 1/1 = major/volatile element analysis; SD, standard deviation
[a] Host is plagioclase

tion. These inclusions were restored to their original composition using the method of Metrich et al. (1991).

The Laki inclusion data are ordered into four groups on the basis of major element abundances (Table 3). Group 1 glass inclusions exhibited major element abundances (Mg# = 42.77 ± 1.37) that closely match the averaged bulk composition of the Laki magma (Mg# = 43.34 ± 0.66) and are considered to be representative of the pre-eruption magma composition. For most inclusions, S concentrations range from 1500 to 1700 ppm (mean 1677 ± 225 ppm), chlorine 250–350 ppm (mean 310 ± 59 ppm), and fluorine 600–800 ppm (mean 665 ± 100 ppm). Group 2 inclusions demonstrate higher Fe and lower Ca and Na contents than those of group 1. However, their mean abundances of S (1632 ± 171 ppm), Cl (246 ± 56 ppm), and F (537 ± 90 ppm) are strikingly similar. The difference in the major element composition cannot be accounted for entirely by host crystallization after entrapment. Group 3 inclusions are strongly enriched in Fe and Ti, depleted in Mg, Ca, and Na, but with volatile concentrations in the same range as the two former groups. Inclusions of groups 2 and 3 may represent liquids which have evolved by fractionation in the Laki reservoir. Group 4 inclusions have an olivine tholeiite composition and may represent a parental liquid to the Laki magma.

The S, Cl, and F values of Laki inclusions have some degree of variance (Fig. 6), which cannot be attributed to analytical error alone. This variance could be caused by several factors: (a) compositional heterogeneity in the magma reservoir; (b) a fraction of the volatiles may have separated from the liquid phase into a bubble within the inclusions as the system was decompressed;

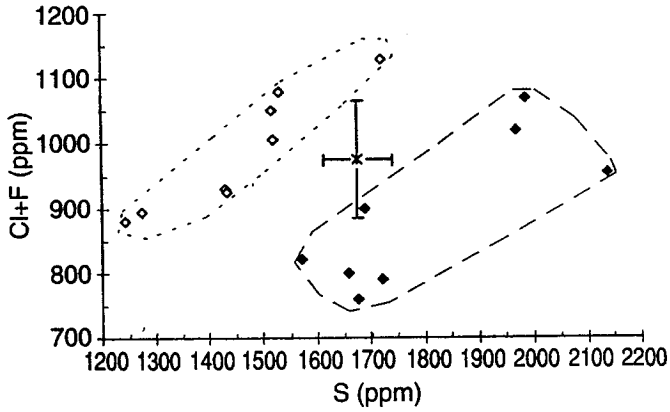


**Fig. 6** Halogen-sulfur covariation diagram for Laki glass inclusions. Inclusions with low (Cl + F)/S values (*filled diamonds*) are outlined by the *heavy broken line*, whereas the *light broken line* outlines inclusions with high (Cl + F)/S values (*open diamonds*). The average inclusion value is shown by the *asterisk* and the *bars* indicate the estimated analytical error ($2\sigma$)

and (c) S-, Cl-, and/or F-bearing mineral phases may have formed in some inclusions after entrapment, although the major element concentrations and petrographic examination reveal no evidence of such minerals. Despite the relatively random distribution of data points in Fig. 6, the data appear to form two arrays, one with low (0.45–0.54) and another with high (0.64–0.71) halogen-to-sulfur ratios. Vapor bubbles are not present in inclusions with low (Cl + F)/S values, whereas many, but not all, of the inclusions with high (Cl + F)/S values contain vapor bubbles. The apparent association of vapor bubbles and low S values in some Laki inclusions may suggest that S (along with $CO_2$ and $H_2O$?) was exsolved from the inclusion melt to form bubbles contain-

**Table 4** Composition of groundmass glass in Laki tephra clasts

| Fall Unit | $SiO_2$ | $TiO_2$ | $Al_2O_3$ | FeO | MnO | MgO | CaO | $Na_2O$ | $K_2O$ | $P_2O_5$ | Sum | S | Cl | F | Mg# | Ves.% | Cr.% | *N* |
|---|---|---|---|---|---|---|---|---|---|---|---|---|---|---|---|---|---|---|
| **Strombolian tephra** | | | | | | | | | | | | | | | | | | |
| S1 | 50.06 | 3.06 | 13.22 | 14.31 | 0.21 | 5.43 | 9.87 | 2.80 | 0.45 | 0.32 | 99.74 | 453 | 205 | 480 | 40.35 | 59 | 2 | 29/23 |
| SD | 0.19 | 0.06 | 0.09 | 0.23 | 0.04 | 0.07 | 0.15 | 0.09 | 0.02 | 0.05 | 0.23 | 78 | 48 | 85 | 0.50 | 19 | 1 | |
| S2 | 49.95 | 3.05 | 13.29 | 14.34 | 0.25 | 5.38 | 10.01 | 2.81 | 0.48 | 0.35 | 99.71 | 513 | 148 | 480 | 40.05 | 45 | 4 | 6/5 |
| SD | 0.16 | 0.06 | 0.11 | 0.33 | 0.02 | 0.08 | 0.16 | 0.05 | 0.02 | 0.01 | 0.41 | 21 | 11 | 53 | 0.83 | 11 | 1 | |
| S3 | 49.80 | 3.01 | 13.19 | 14.03 | 0.21 | 5.41 | 9.87 | 2.72 | 0.45 | 0.30 | 98.98 | 515 | 256 | 472 | 40.51 | 77 | 1 | 30/36 |
| SD | 0.34 | 0.04 | 0.11 | 0.25 | 0.03 | 0.05 | 0.10 | 0.15 | 0.02 | 0.04 | 0.44 | 88 | 77 | 99 | 0.41 | 10 | 0 | |
| S4 | 50.07 | 3.14 | 13.08 | 14.42 | 0.24 | 5.21 | 10.10 | 2.83 | 0.49 | 0.36 | 99.93 | 473 | 149 | 491 | 39,16 | 27 | 4 | 6/6 |
| SD | 0.11 | 0.04 | 0.06 | 0.15 | 0.03 | 0.04 | 0.05 | 0.05 | 0.02 | 0.01 | 0.26 | 26 | 20 | 64 | 0.12 | 2 | 2 | |
| S1–S4 | | | | | | | | | | | | | | | | | | |
| Average | 49.94 | 3.05 | 13.20 | 14.20 | 0.22 | 5.40 | 9.90 | 2.77 | 0.45 | 0.32 | 99.43 | 490 | 223 | 476 | 40.39 | 64 | 2 | 71/70 |
| SD | 0.28 | 0.06 | 0.11 | 0.28 | 0.03 | 0.09 | 0.15 | 0.12 | 0.03 | 0.05 | 0.52 | 82 | 74 | 89 | 0.64 | 20 | 1 | |
| **Phreatomagmatic tephra** | | | | | | | | | | | | | | | | | | |
| P1 | 49.66 | 2.84 | 13.34 | 13.80 | 0.22 | 5.74 | 10.71 | 2.40 | 0.56 | 0.26 | 99.53 | 937 | 218 | 421 | 42.56 | 33 | 4 | 32/54 |
| SD | 0.25 | 0.14 | 0.14 | 0.35 | 0.03 | 0.26 | 0.55 | 0.21 | 0.10 | 0.04 | 0.38 | 217 | 79 | 106 | 1.57 | 31 | 4 | |
| P2 | 49.84 | 2.78 | 13.48 | 13.60 | 0.22 | 5.70 | 10.68 | 2.77 | 0.42 | 0.31 | 99.81 | 903 | 133 | 418 | 42,74 | 36 | 1 | 9/7 |
| SD | 0.27 | 0.30 | 0.20 | 0.78 | 0.03 | 0.57 | 0.76 | 0.15 | 0.07 | 0.05 | 0.33 | 176 | 24 | 64 | 3.77 | 35 | 1 | |
| P1–P2 | | | | | | | | | | | | | | | | | | |
| Average | 49.70 | 2.83 | 13.37 | 13.75 | 0.22 | 5.73 | 10.70 | 2.48 | 0.53 | 0.27 | 99.59 | 933 | 208 | 420 | 42.60 | 34 | 3 | 41/61 |
| SD | 0.26 | 0.18 | 0.16 | 0.47 | 0.03 | 0.34 | 0.59 | 0.25 | 0.11 | 0.04 | 0.38 | 212 | 79 | 102 | 2.18 | 31 | 4 | |

Individual fall units are designated as in Thordarson and Self (1993). S, strombolian tephra units; P, phreatomagmatic tephra units; Mg# = 100 Mg/(Mg+Fe*), Fe* = total Fe; Ves% and Cr.%, vesicle and crystal content of sample in vol. %, respectively, *N*, number of analyses – 1/1 = major/volatile element analyses; SD, standard deviation ($2\sigma$)

ing a free volatile phase as the magma rose to the surface, although more work is necessary to confirm this relationship. Consequently, the mean S concentration of group 1 inclusions (Table 3) is likely to be a minimum estimate for dissolved sulfur in the Laki magma prior to eruption. The variance in volatile concentrations demonstrates clearly the importance of analyzing multiple inclusions to obtain a reasonable estimate of pre-eruption volatile concentrations.

## Vent tephra

The Laki fall deposits consist of holohyaline tephra clasts with sparse phenocrysts (1–10 vol.%) of olivine, plagioclase, and clinopyroxene. Although the analyzed tephra represents fall units produced by episodic explosive activity over a period of 3 months (Fig. 2), the major element composition of their groundmass glass show no systematic variations with stratigraphic position (Table 4). However, the major element data indicate a slight compositional difference between groundmass glass of the two types of tephra produced by the eruption, identified as two partly overlapping fields on bivariate plots (Fig. 7). The strombolian tephra has higher FeO and $TiO_2$, but lower MgO than the bulk magma, and is slightly more evolved. The dense clustering of data points confirms the uniform composition of all strombolian fall units. The groundmass glass of the phreatomagmatic clasts shows more variable major element concentrations, forming an array spanning the

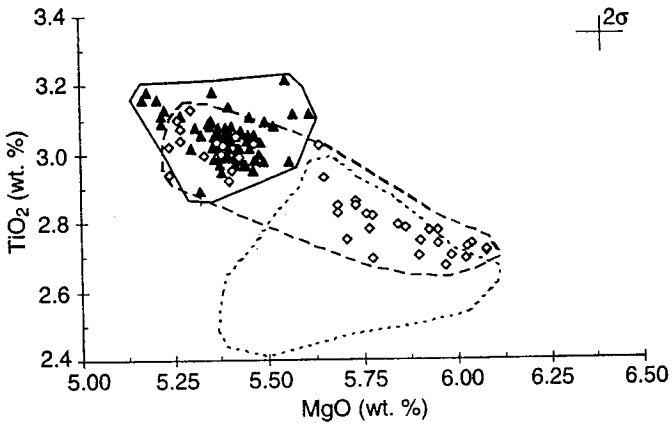


**Fig. 7** Compositional variations in Laki tephra samples. $TiO_2$ (wt.%) as a function of MgO (wt.%). Note the strong clustering exhibited by the strombolian tephra (*filled triangles*) and the rough linear trend defined by the phreatomagmatic tephra (*open diamonds*). *Solid* and *broken lines* outline the compositional fields of strombolian and phreatomagmatic tephra, respectively. *Dotted line* defines the whole-rock compositional field of Laki eruption products. Estimated analytical error ($2\sigma$) is shown by the *cross* in the upper right corner

compositional range of the bulk magma and the strombolian tephra. Nevertheless, a majority of the clasts resemble the bulk magma composition (Fig. 7).

The variable, but high, S concentration in groundmass glass of phreatomagmatic clasts (mean 933 ± 212 ppm) contrasts with very uniform S abundances in the strombolian clasts (mean 490 ± 82 ppm).

The S values of the phreatomagmatic tephra range from approximately 1260 to 490 ppm, but the corresponding compositional range for the strombolian tephra is 418–640 ppm S (Table A-1, Appendix II). The groundmass glass of both tephra types have variable, but similar, Cl and F concentrations. However, the compositional range of Cl and F is greater in phreatomagmatic tephra (Cl = 122–450 ppm; F = 220–560 ppm) than in the strombolian tephra (Cl = 134–320 ppm; F = 310–530 ppm).

The compositional differences and similarities between the two tephra types are of interest because the tephras represent different styles of explosive activity. The strombolian tephra deposits formed as the melt was disintegrated by rapidly expanding magmatic gases, whereas the phreatomagmatic tephra was produced by interaction of external water and magma (Thordarson and Self 1993). The strombolian tephra units are composed of well-sorted scoria lapilli, consisting primarily of highly vesicular clasts (60–90 vol.% voids) featuring a single population of 2- to 10-mm spherical vesicles. The strombolian clasts are either partly or wholly coated by a thin fluidal skin (<0.01 mm), suggesting that the outer surfaces of the clasts were fused (Fig. 8a and b), presumably by a stream of hot gas. The strombolian tephra also contains reticulite and Pele's hair. The phreatomagmatic tephra units are composed of poorly sorted ash to scoria lapilli consisting of non-vesicular to highly vesicular angular clasts (Fig. 8c) in approximately equal proportions. The phreatomagmatic clasts lack the glassy fluidal skin that characterizes the strombolian tephra clasts. The highly vesicular clasts in both tephra types represent true magmatic foam, and the reticulite-like strombolian clasts indicate that a small fraction of the melt had evolved to mature polyhedral foam (Cashman and Mangan 1994).

Major element abundances in both tephra types show poor correlation with clast vesicularity, although higher vesicle abundance (>45 vol.%) appears to accompany a more evolved (iron-rich) composition (Fig. 9a). S abundances in the groundmass glass of phreatomagmatic clasts show a weak negative correlation with degree of vesicularity, whereas the S concentrations in strombolian clasts are independent of vesicle abundance (Fig. 9b). Furthermore, the fluorine and chlorine concentrations show no obvious correlation with vesicularity (Fig. 9c). Considering the nature and timing of eruptive events and the relatively small tephra volume, the more evolved tephra compositions suggest that a portion of the magma fractionated chemically during its rise to the surface.

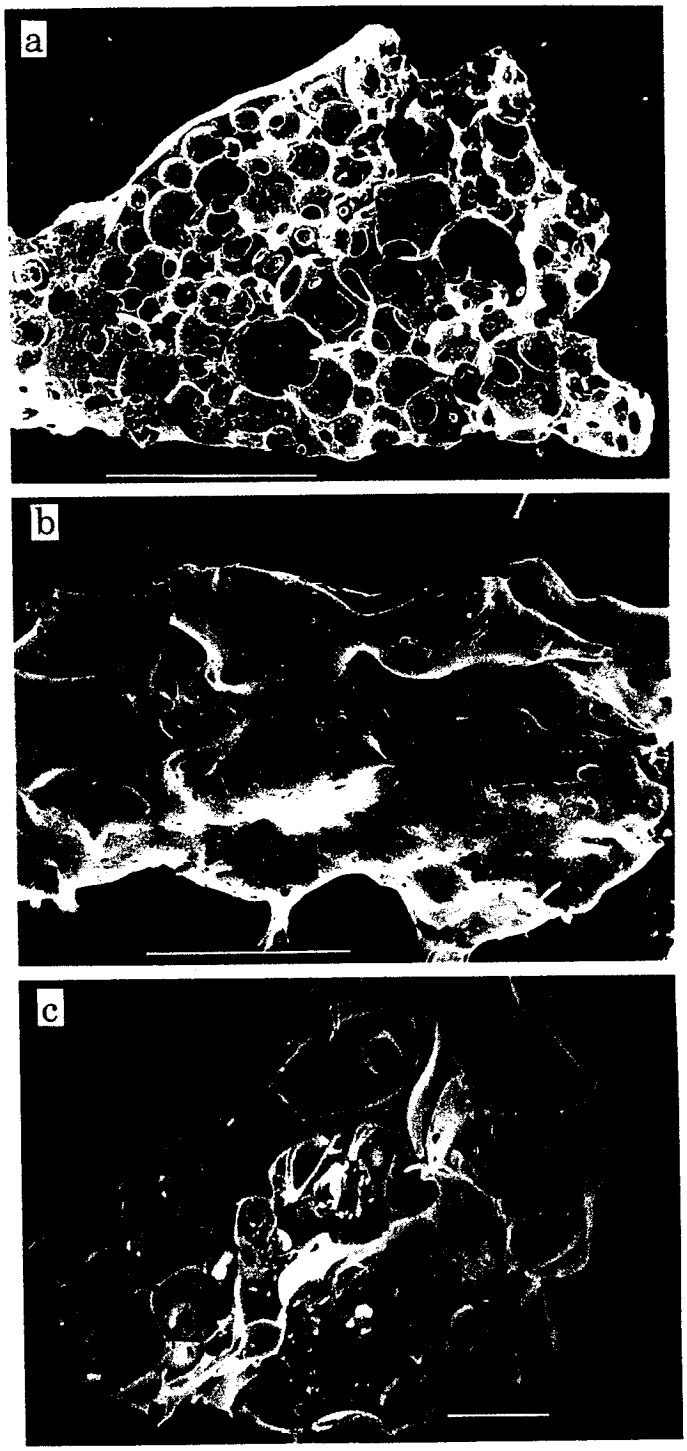


**Fig. 8a–c** Scanning electron photomicrographs of highly vesicular (foam-like) tephra particles from Laki. **a** Interior of a clast from the strombolian tephra deposit. Scale bar is 1000 μm (*white line*). **b** Strombolian clast completely covered by a very thin fluidal skin. The interior of the clast is highly vesicular (~80 vol.% voids). *Scale bar* is 1000 μm. **c** Clast from the phreatomagmatic tephra deposit. *Scale bar* is 1000 μm

## Lava selvages and rootless-cone tephra

The basal-quenched lava selvages and the rootless-cone tephra exhibit hyalophitic (intersertal) texture, in which glomerocrysts (5–6 vol.%) and the seriate-textured groundmass mineral assemblage of plagioclase, olivine,

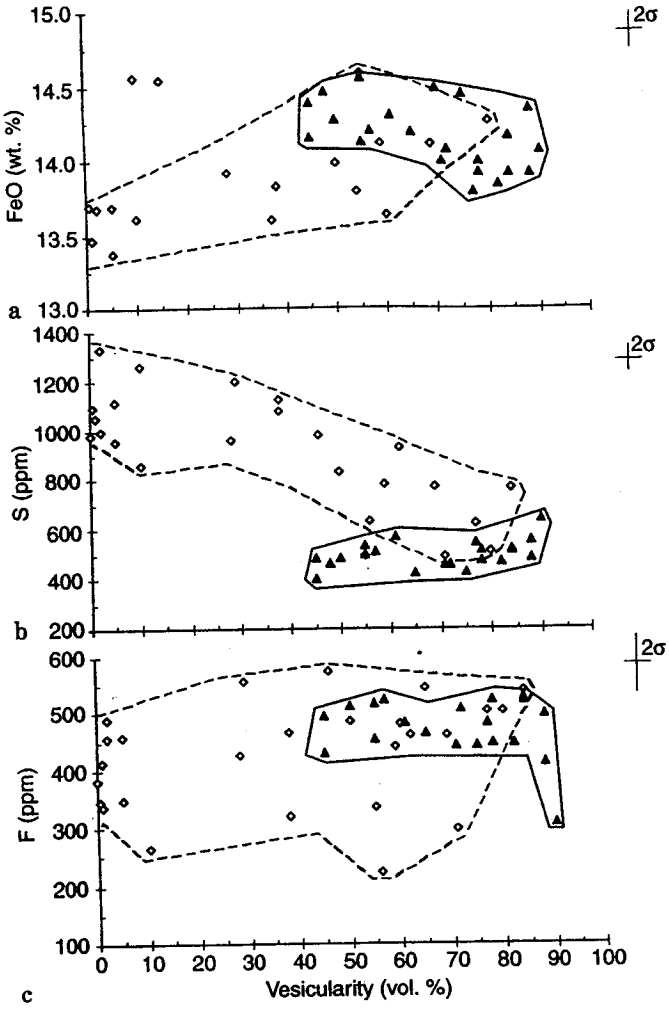


**Fig. 9a–c** Variation in volatile abundances as function of vesicularity in Laki tephra samples. **a** FeO vs vesicularity. **b** S vs vesicularity. **c** F vs vesicularity. Phreatomagmatic tephra is indicated by *open diamonds*, and strombolian tephra by *filled triangles*. Estimated analytical error ($2\sigma$) is shown by the *cross* in the upper right corner

**Fig. 10** Transmitted-light photomicrograph of Laki lava selvage (sample L-21) demonstrating the holohyaline nature of the groundmass and the seriate texture of the mineral assemblage. Note also that no Fe–Ti oxide mineral phases are present. *Scale bar* is 500 μm

and clinopyroxene (~10–40 vol.%) are completely embedded in light- to dark-brown sideromelane glass (Fig. 10). Fe–Ti oxides are not present in the groundmass mineral assemblages of lava selvages and rootless-cone tephra.

The groundmass glass of the lava selvages and the rootless-cone tephra clasts shows a more evolved composition than the bulk lava and tephra (Table 5a). Groundmass glass of proximal lava samples shows the smallest variation from the bulk lava composition, with an Mg# of 35.4±2.2. The groundmass glass of the medial and distal samples, however, shows a considerable degree of differentiation with strong enrichment in $TiO_2$ and FeO, and Mg# between 32.7±1.8 and 34.0±0.2 (Fig. 11a; Table 5a). The S, Cl, and F concentrations of the groundmass glass in the proximal lava are in the same range as that of the strombolian tephra (Tables 4 and 5a). Furthermore, the measured abundances of S (334±29 to 489±5 ppm), Cl (188±49 to 309±98 ppm), and F (495±109 to 613±93) in groundmass glass of lava selvages and rootless-cone tephra from the medial and distal locations (Fig. 11b) are surprisingly uniform and on average similar or only slightly lower than those found in the proximal lava and strombolian tephra.

The crystallinity of lava selvages and rootless-cone tephra ranges from 12 to 50 vol.%, with the least crystalline samples being closest to source (Table AII-1, Appendix II). The crystal content of the lava glass selvages falls between 25 and 38 vol.% and, in general, increases with distance from the source (Fig. 11c). The rootless-cone tephra at Leidólfsfell shows a greater range of crystallinity (30–50 vol.%). Despite the evolved groundmass glass composition, the bulk (whole-rock) composition of the rootless-cone tephra and lava (Table 5b) is essentially the same as the original magma composition. A general negative correlation between Mg# and degree of crystallinity (Fig. 11a and c) implies that the observed differentiation of the groundmass glass is caused by in situ crystallization (or equilibrium crystallization at a constant total composition) of the liquid lava during emplacement. If we take the whole-rock composition of the rootless-cone tephra as the starting liquid composition and allow ~30% crystallization of the observed groundmass mineral assemblage in lava selvages and rootless-cone tephra (plagioclase, augite, and olivine in the fractions of 0.4, 0.4, and 0.2, respectively), the calculated liquid composition agrees with the mean composition of the rootless-cone groundmass glass (Table 5b). The absence of Fe-Ti oxides from the groundmass mineral assemblage of these samples is consistent with the strong FeO and $TiO_2$ enrichment observed in the groundmass glass and implies that the emplacement temperatures of the lava were above the Fe–Ti oxides liquidus temperatures. The concentrations of S, Cl, and F gradually increase in the remaining liquid as crystallization progresses be-

**Table 5a** Composition of groundmass glass in Laki lava selvages and rootless cone tephra (RCT) at proximal, medial and distal locations in the Laki lava field. Also shown are average whole-rock composition of rootless cone tephra and crystalline lava (Cr. lava)

| | $SiO_2$ | $TiO_2$ | $Al_2O_3$ | FeO | MnO | MgO | CaO | $Na_2O$ | $K_2O$ | $P_2O_5$ | Sum | S | Cl | F | Mg# | Cr.% | *N* |
|---|---|---|---|---|---|---|---|---|---|---|---|---|---|---|---|---|---|
| **Proximal** | | | | | | | | | | | | | | | | | |
| RCT-gm | 49.61 | 3.61 | 12.37 | 15.62 | 0.24 | 4.80 | 9.89 | 2.70 | 0.57 | 0.44 | 99.84 | 480 | 167 | 416 | 35.40 | 20 | 23/24 |
| SD | 0.53 | 0.36 | 0.56 | 0.83 | 0.03 | 0.25 | 0.19 | 0.19 | 0.14 | 0.15 | 0.24 | 201 | 58 | 55 | 2.16 | 11 | |
| Cr. lava-wr[a] | 50.15 | 2.84 | 13.72 | 13.65 | 0.21 | 5.61 | 10.40 | 2.51 | 0.43 | 0.32 | 99.84 | | | | 42.26 | | 7 |
| SD | 0.21 | 0.09 | 0.17 | 0.22 | 0.00 | 0.09 | 0.04 | 0.11 | 0.01 | 0.04 | 0.20 | | | | 0.76 | | |
| **Medial** | | | | | | | | | | | | | | | | | |
| Lava selvage | 49.99 | 3.84 | 11.82 | 16.11 | 0.25 | 4.64 | 9.44 | 2.77 | 0.58 | 0.37 | 99.82 | 356 | 240 | 494 | 33.92 | 25 | 94/53 |
| SD | 0.27 | 0.10 | 0.21 | 0.34 | 0.04 | 0.14 | 0.21 | 0.14 | 0.11 | 0.07 | 0.46 | 40 | 73 | 108 | 0.93 | 5 | |
| RCT-gm | 49.69 | 3.97 | 11.66 | 16.69 | 0.24 | 4.54 | 9.30 | 2.73 | 0.58 | 0.47 | 99.85 | 275 | 168 | 390 | 32.67 | 38 | 33/27 |
| SD | 0.16 | 0.18 | 0.14 | 0.52 | 0.02 | 0.24 | 0.17 | 0.07 | 0.04 | 0.08 | 0.22 | 37 | 31 | 20 | 1.80 | 9 | |
| RCT-wr | 49.42 | 2.73 | 13.40 | 13.88 | 0.23 | 5.95 | 10.64 | 2.69 | 0.51 | 0.41 | 99.86 | | | | 43.30 | 35 | 3 |
| SD | 0.30 | 0.07 | 0.11 | 0.20 | 0.01 | 0.12 | 0.21 | 0.05 | 0.02 | 0.01 | 0.01 | | | | 0.81 | 10 | |
| Cr. lava-wr[a] | 49.81 | 2.65 | 13.62 | 13.48 | 0.23 | 5.88 | 10.50 | 2.77 | 0.43 | 0.37 | 99.73 | | | | 43.73 | | 3 |
| SD | 0.24 | 0.07 | 0.43 | 0.45 | 0.01 | 0.07 | 0.16 | 0.15 | 0.05 | 0.10 | 0.15 | | | | 0.56 | | |
| **Distal** | | | | | | | | | | | | | | | | | |
| Lava selvage | 49.78 | 3.81 | 11.81 | 16.19 | 0.28 | 4.69 | 9.37 | 2.70 | 0.55 | 0.37 | 99.54 | 340 | 159 | 438 | 34.03 | 37 | 9/21 |
| SD | 0.19 | 0.05 | 0.12 | 0.09 | 0.02 | 0.04 | 0.08 | 0.05 | 0.02 | 0.03 | 0.33 | 14 | 21 | 55 | 0.28 | 1 | |
| Cr. lava-wr[a] | 49.74 | 2.76 | 13.84 | 13.57 | 0.23 | 5.83 | 10.44 | 2.67 | 0.44 | 0.32 | 99.84 | 195 | 150 | 320 | 43.35 | | 6/2 |
| SD | 0.66 | 0.10 | 0.14 | 0.34 | 0.01 | 0.19 | 0.15 | 0.13 | 0.02 | 0.06 | 0.30 | | | | 1.10 | | |

gm, groundmass; wr, whole-rock; Mg# = 100 mg/(Mg + Fe*), Fe* = total Fe; *N*, number of analyses – 1/1 = major/volatile element analyses; SD, standard deviation ($2\sigma$); Cr.%, crystal content of sample in vol. %

[a] Average composition of crystalline lava derived from published whole-rock analyses compiled by Thordarson (1955)

**Table 5b** Crystal fractionation calculations using whole-rock composition of rootless cone tephra as starting liquid composition (see text for further details)

| | $SiO_2$ | $TiO_2$ | $Al_2O_3$ | FeO | MnO | MgO | CaO | $Na_2O$ | $K_2O$ | $P_2O_5$ | Sum | Mg# |
|---|---|---|---|---|---|---|---|---|---|---|---|---|
| RCT-wr | 49.42 | 2.73 | 13.40 | 13.88 | 0.23 | 5.95 | 10.64 | 2.69 | 0.51 | 0.41 | 99.86 | 43.30 |
| Calc comp[a] | 50.60 | 3.72 | 10.86 | 16.73 | 0.31 | 4.55 | 8.85 | 3.04 | 0.53 | 0.56 | 99.75 | 32.65 |
| RCT-gm | 49.69 | 3.97 | 11.66 | 16.69 | 0.24 | 4.54 | 9.30 | 2.73 | 0.58 | 0.47 | 99.85 | 32.67 |

[a] Crystallization required: 29%. gm, groundmass; wr, whole-rock

cause these elements are incompatible with the crystallizing phases. This simple chemical process is complicated by the fact that the lava loses a fraction of these elements (especially S) through degassing, but at the same time the strong FeO enrichment is likely to increase the solubility of sulfur in the liquid lava (Haughton et al. 1974). Consequently, to find the representative concentration of these elements in the bulk lava (the original liquid after vent degassing) it is necessary to correct for the amount of crystallization which occurred during lava transport. When corrected, the S, Cl, and F values of samples from the medial and distal part of the lava still show remarkable uniformity (Fig. 11b; Table A-2, Appendix II).

## Geothermometry

Because of the temperature dependence of sulfur solubility and magma rheology, and the long duration of the Laki eruption, it is important to evaluate the variations in melt temperatures during the eruption. One-atmosphere melting experiments performed on Laki lava samples suggest that magma-reservoir temperatures were at least 1150±10 °C (Bell and Humphries 1972), and that lava-emplacement temperatures were above 1085 °C (Thordarson 1995). From the empirical glass geothermometer of Helz and Thornber (1987), inclusion chemistry indicates magmatic temperatures near 1140 ± 8 °C (Fig. 12).

We estimate the melt temperature of Laki tephra and lava on the basis of MgO and CaO concentrations of groundmass glasses (Helz and Thornber 1987), which is justified by the linear co-variations of these elements (Thordarson 1995). The calculated MgO- and CaO temperatures agree and are internally consistent. The CaO-derived temperatures give, on average, slightly higher values which may be attributed to the difference in the crystallization sequence between the Laki magma (plagioclase–olivine–clinopyroxene) and the

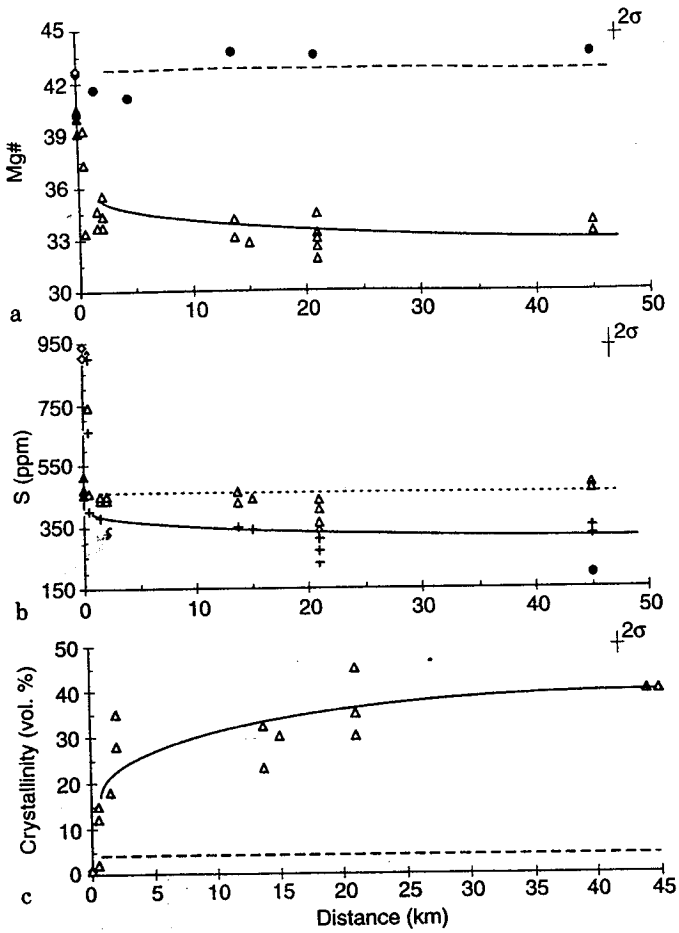


**Fig. 11a–c** Variation in Mg#, S, and crystallinity with distance from source. Lava selvages and rootless-cone tephras are indicated by *open triangles*, strombolian tephra by *filled triangles*, phreatomagmatic tephra by *open diamonds*, and crystalline lava by *filled circles*. **a** Mg# vs distance. *Solid line* indicates the inferred change in Mg# of lava selvage with distance and *broken line* changes in Mg# of crystalline lava. **b** S vs distance. *Broken* and *solid line* indicate inferred changes in measured and corrected S abundances (*plusses*), respectively, of lava selvages with distance. **c** Crystallinity of lava selvages and rootless-cone tephras with distance from source. *Solid line* indicates the inferred changes in crystal content of lava selvage with distance; *broken line* indicates the pre-eruption crystal content of the Laki magma. Estimated analytical error ($2\sigma$) is shown by the *cross* in the upper right corner

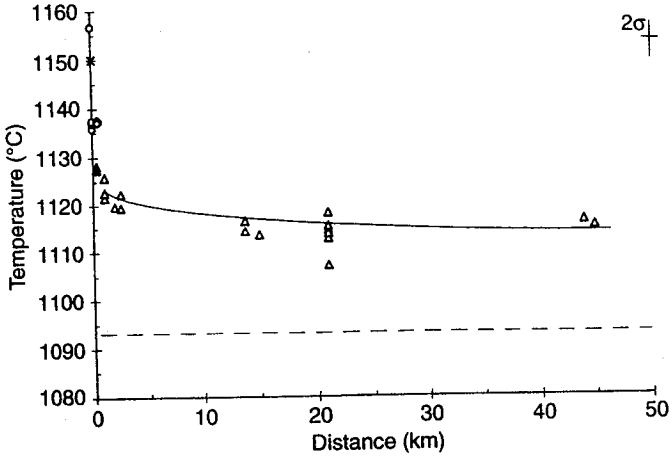


**Fig. 12** Laki magma and liquid lava temperatures as a function with distance from source. Temperatures were calculated according to the empirical geothermometer of Helz and Thornber (1987). *Cross* indicates liquidus temperature of the Laki magma as determined by 1-atm melting experiments (Bell and Humphries 1972). Laki inclusions are indicated by *open circles*, phreatomagmatic tephra by *open diamonds*, and strombolian tephra and lava selvages by *filled* and *open triangles*, respectively. Inferred change in lava temperature with distance from source is indicated by *the solid line*. *Broken line* shows the liquidus temperature of FeTi-oxides in the Laki magma. Estimated analytical error ($2\sigma$) is shown by the cross in the upper right corner

Kilauea Iki lava lake magma (olivine–clinopyroxene–plagioclase) used for geothermometer calibration. The geothermometer calculations indicate that the melt temperature of the phreatomagmatic tephra was $1138 \pm 9$ °C at the time of explosive interaction of magma and external water (Fig. 12), whereas the temperature of strombolian tephra was $\sim 1127 \pm 3$ °C upon melt disintegration. The results suggest that quenching and fragmentation of the phreatomagmatic tephra occurred at greater depth in the feeder dikes. Furthermore, the high melt temperatures of the phreatomagmatic tephra suggest that cooling during ascent had insignificant, if any, effects on the flow regime within the feeder dike. The calculated emplacement temperature for the proximal lava ranges from 1120 to 1126 °C and is similar to that of the strombolian tephra. Temperatures obtained from samples of the medial and distal lavas are 10–20 °C lower (1107–1117 °C) and show no obvious variation with distance from source (Fig. 12), indicating that lava transport was thermally efficient.

## Estimates of volatile release by the Laki eruption

### Methodology

Several studies (Rose 1977; Óskarsson et al. 1984; Devine et al. 1984) have demonstrated clearly the validity of a petrologic approach to evaluate the potential atmospheric sulfur yield from eruptions, although the applicability of the method may depend on the pre-eruption condition in the magma source region. For example, Wallace and Gerlach (1994) and Gerlach et al. (1994) argue that the petrologic method underestimates the $SO_2$ flux from andesite–dacite eruptions at convergent margin volcanoes, because the magma carries the bulk of the sulfur in an accumulated vapor phase. It should be noted, however, that these convergent margin magmas are hybrids residing in shallow crustal magma chambers, and that their pre-eruption evolution is complicated by incomplete magma mixing, crystallization, and fractionation (e.g., Nye et al. 1994).

The large volume and homogeneous composition of the Laki products imply that they were erupted from a compositionally uniform magma body in a deep-seated (>10 km) reservoir at the base of the crust below Ice-

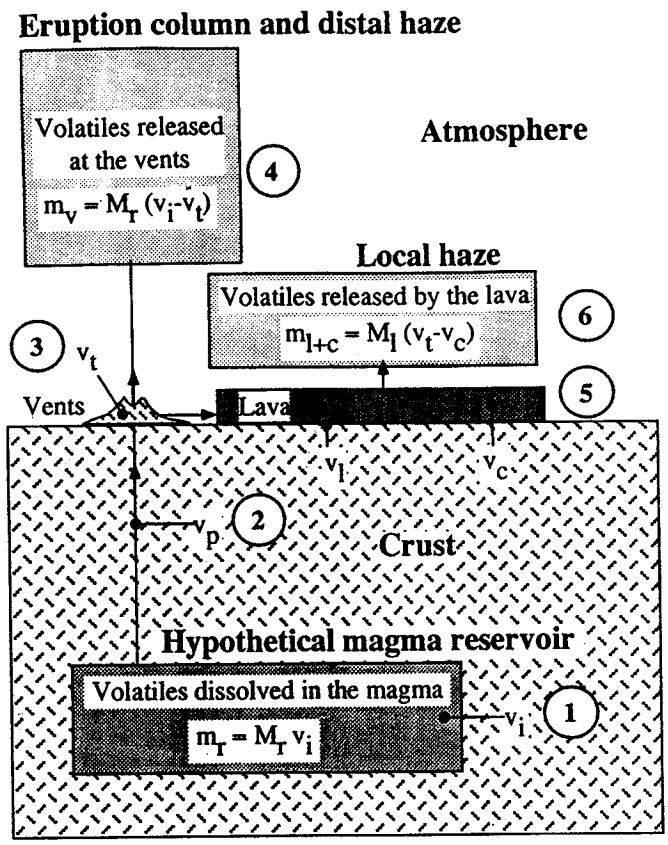


**Fig. 13** Illustration outlining a volatile budget model for basaltic fissure eruptions. *1* Hypothetical magma reservoir containing magma of the mass $M_r$ (taken here to be equal to erupted volume of magma) and total amount of dissolved volatiles $m_r$; the measured concentration of volatiles in glass inclusions, $v_i$, represents the concentration of volatiles dissolved in the magma. The total mass of volatiles dissolved in the magma prior to eruption is given by the lowermost equation. *2* Quenched magma fraction due to interaction with external water, represented by phreatomagmatic tephra at the surface containing volatile concentrations $v_p$. *3* Vent accumulations of pyroclastic material containing concentrations of volatiles $v_t$, which represents volatile fraction of $m_r$ which did not escape the magma as it emerged from the vents. *4* Eruption column (lava fountain plus convecting plume) containing total amount of volatiles released at the vents, $m_v$, as given by the uppermost equation. *5* Lava flow of mass $M_l$ and volatile concentration $v_l$ in lava selvages and $v_c$ in crystalline lava. *6* Amount of volatiles, $m_{l+c}$, released by the degassing of lava during and after emplacement is given by the middle equation

land (Sigmarsson et al. 1991). Based on the chemical similarities between group-1 inclusions and the erupted products (Table 3), we conclude that the inclusions represent the pre-eruption Laki magma. The high volatile concentrations in the inclusions compared with concentrations in groundmass glass of quenched eruption products supports this conclusion. Therefore, we use the petrologic method, modified from Óskarsson et al. (1984) and Devine et al. (1984), to estimate the volatile yield of the Laki eruption.

In fissure eruptions, such as Laki, the release of volatiles by the magma can be viewed as occurring in two main stages (Fig. 13): (a) vent degassing of magma during strombolian explosive activity or Hawaiian-type lava-fountaining; and (b) degassing of magma during and after flow of lava. Thus, it should be possible to obtain information on the degree of degassing during an eruption by comparing the pre-eruption volatile content to the content of volatiles retained in the products of each phase, although the crystallization of magma as it passes through each stage must be accounted for. The volatile concentrations in rapidly cooled pyroclasts and glassy selvages of proximal lavas are indicators of the amount retained by the magma as it flowed away from the vents. Glass selvages from the base of lava flow units and tephra clasts from the rootless cone deposits indicate the residual amount of volatiles in molten lava upon emplacement at some distance from source. Volatile contents of crystalline lavas represent the final residue of gases which did not escape from the lava into the atmosphere.

Assuming that the total mass erupted equals the mass of magma that contributes to the volatile emission during the eruption, then the volatile budget of the eruption can be schematically modeled as illustrated in Fig. 13. The total mass ($m_r$) of single volatile species ($x$) dissolved in magma residing in a reservoir ($r$) at depth and effectively involved in the eruption is:

$$m_{x,r} = M_r v_{x,i}$$

where $M_r$ is mass of magma which is degassed effectively during the eruption and $v_{x,i}$ is the mass fraction of a gaseous element $x$ in inclusions ($i$). The total mass ($m_{x,v}$) of each volatile species which escapes from the magma at the vents ($v$) and is dispersed into the atmosphere by the eruption column is estimated by:

$$m_{x,v} = (v_{x,i} - v_{x,t}) M_r$$

where $v_{x,t}$ is the average mass fraction of the gaseous species $x$ in strombolian tephra and proximal lava ($t$). Similarly, the mass released into the atmosphere from the lava during emplacement ($m_{x,l}$) and after emplacement ($m_{x,c}$) is estimated according to:

$$m_{x,l} = (v_{x,t} - v_{x,l}) M_l$$
$$m_{x,c} = (v_{x,l} - v_{x,c}) M_l$$

where $v_{x,l}$ and $v_{x,c}$ are the mass fraction of the gaseous species $x$ in glassy lava selvages and crystalline lava, respectively, and $M_l$ is the total mass of lava.

## Application

The data used to calculate the volatiles released in various stages of the Laki eruption are presented in Table 6. The mass of each volatile species carried to the surface by the erupting magma is calculated by:

$$m_{x,r} = M_r v_{x,i} = V_r \rho \varepsilon v_{x,i}$$

where $V_r$ is total erupted volume taken as 15.1 $km^3$ (Thordarson and Self 1993), $\rho$ is the magma density, 2750 kg $m^{-3}$ (Metrich et al. 1991), $v_{x,i}$ is the mass fraction of individual elements in glass inclusions, and $\varepsilon$ is

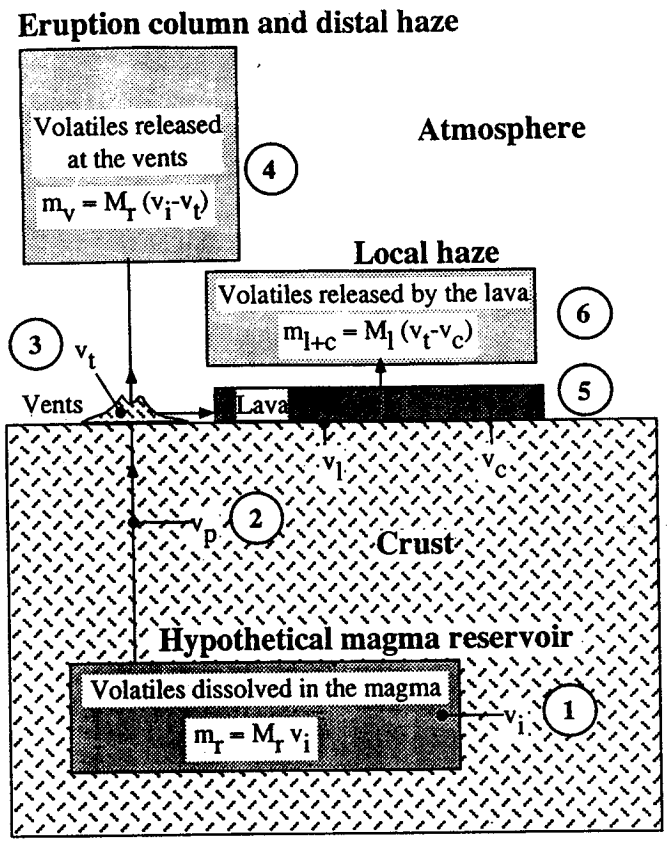


**Fig. 13** Illustration outlining a volatile budget model for basaltic fissure eruptions. *1* Hypothetical magma reservoir containing magma of the mass $M_r$ (taken here to be equal to erupted volume of magma) and total amount of dissolved volatiles $m_r$; the measured concentration of volatiles in glass inclusions, $v_i$, represents the concentration of volatiles dissolved in the magma. The total mass of volatiles dissolved in the magma prior to eruption is given by the lowermost equation. *2* Quenched magma fraction due to interaction with external water, represented by phreatomagmatic tephra at the surface containing volatile concentrations $v_p$. *3* Vent accumulations of pyroclastic material containing concentrations of volatiles $v_t$, which represents volatile fraction of $m_r$ which did not escape the magma as it emerged from the vents. *4* Eruption column (lava fountain plus convecting plume) containing total amount of volatiles released at the vents, $m_v$, as given by the uppermost equation. *5* Lava flow of mass $M_l$ and volatile concentration $v_l$ in lava selvages and $v_c$ in crystalline lava. *6* Amount of volatiles, $m_{l+c}$, released by the degassing of lava during and after emplacement is given by the middle equation

land (Sigmarsson et al. 1991). Based on the chemical similarities between group-1 inclusions and the erupted products (Table 3), we conclude that the inclusions represent the pre-eruption Laki magma. The high volatile concentrations in the inclusions compared with concentrations in groundmass glass of quenched eruption products supports this conclusion. Therefore, we use the petrologic method, modified from Óskarsson et al. (1984) and Devine et al. (1984), to estimate the volatile yield of the Laki eruption.

In fissure eruptions, such as Laki, the release of volatiles by the magma can be viewed as occurring in two main stages (Fig. 13): (a) vent degassing of magma during strombolian explosive activity or Hawaiian-type lava-fountaining; and (b) degassing of magma during and after flow of lava. Thus, it should be possible to obtain information on the degree of degassing during an eruption by comparing the pre-eruption volatile content to the content of volatiles retained in the products of each phase, although the crystallization of magma as it passes through each stage must be accounted for. The volatile concentrations in rapidly cooled pyroclasts and glassy selvages of proximal lavas are indicators of the amount retained by the magma as it flowed away from the vents. Glass selvages from the base of lava flow units and tephra clasts from the rootless cone deposits indicate the residual amount of volatiles in molten lava upon emplacement at some distance from source. Volatile contents of crystalline lavas represent the final residue of gases which did not escape from the lava into the atmosphere.

Assuming that the total mass erupted equals the mass of magma that contributes to the volatile emission during the eruption, then the volatile budget of the eruption can be schematically modeled as illustrated in Fig. 13. The total mass ($m_r$) of single volatile species ($x$) dissolved in magma residing in a reservoir ($r$) at depth and effectively involved in the eruption is:

$$m_{x,r} = M_r v_{x,i}$$

where $M_r$ is mass of magma which is degassed effectively during the eruption and $v_{x,i}$ is the mass fraction of a gaseous element $x$ in inclusions ($i$). The total mass ($m_{x,v}$) of each volatile species which escapes from the magma at the vents ($v$) and is dispersed into the atmosphere by the eruption column is estimated by:

$$m_{x,v} = (v_{x,i} - v_{x,t}) M_r$$

where $v_{x,t}$ is the average mass fraction of the gaseous species $x$ in strombolian tephra and proximal lava ($t$). Similarly, the mass released into the atmosphere from the lava during emplacement ($m_{x,l}$) and after emplacement ($m_{x,c}$) is estimated according to:

$$m_{x,l} = (v_{x,t} - v_{x,l}) M_l$$
$$m_{x,c} = (v_{x,l} - v_{x,c}) M_l$$

where $v_{x,l}$ and $v_{x,c}$ are the mass fraction of the gaseous species $x$ in glassy lava selvages and crystalline lava, respectively, and $M_l$ is the total mass of lava.

## Application

The data used to calculate the volatiles released in various stages of the Laki eruption are presented in Table 6. The mass of each volatile species carried to the surface by the erupting magma is calculated by:

$$m_{x,r} = M_r v_{x,i} = V_r \rho \varepsilon v_{x,i}$$

where $V_r$ is total erupted volume taken as 15.1 km$^3$ (Thordarson and Self 1993), $\rho$ is the magma density, 2750 kg m$^{-3}$ (Metrich et al. 1991), $v_{x,i}$ is the mass fraction of individual elements in glass inclusions, and $\varepsilon$ is

**Table 6**

**a) Averaged concentration (in ppm) of volatile species in the Laki eruption products**

| | S | Cl | F | $H_2O$ | $CO_2$ | Σ |
|---|---|---|---|---|---|---|
| *Inclusions* | | | | | | |
| Laki type ($v_i$) | 1675 ±225 | 310 ±59 | 665 ±100 | 6325[a] | *8530*[a] | 17505 |
| *Tephra* | | | | | | |
| Strombolian ($v_t$) | 490 ±82 | 225 ±74 | 475 ±89 | 1915[a] | *1480*[a] | 4615 |
| *Lava* | | | | | | |
| Lava selvage ($v_l$) | 350 ±30 | 185 ±55 | 435 ±80 | | | |
| Crystalline lava ($v_c$) | 195[a] | 150[a] | 315[a] | 620[a] | 100[a] | 1380 |
| *Total in solidified eruption products* | | | | | | |
| Lava + tephra ($v_s$) | 205 ±10 | 150 ±5 | 320 ±10 | 655 | 135 | 1465 |

**b) Volatile abundances (in ppm) used in calculating the amount released by various eruption stages**

| | ΔS | ΔCl | ΔF | $\Delta H_2O$ | $\Delta CO_2$ | ΔΣ |
|---|---|---|---|---|---|---|
| Total amount released ($v_i$–$v_s$) | 1470 | 160 | 345 | 5670 | 8395 | 16040 |
| Amount released at vents ($v_i$–$v_t$) | 1185 | 85 | 190 | 4410 | 7050 | 12890 |
| Amount released during lava transport ($v_t$–$v_l$) | 140 | 40 | 40 | – | – | – |
| Amount released after lava emplacement ($v_l$–$v_c$) | 155 | 35 | 115 | 1260[b] | 1345[b] | 3165[b] |

**c) Estimates on degree (%) of magma degassing at various eruption stages**

| | S | Cl | F | $H_2O$ | $CO_2$ | Σ |
|---|---|---|---|---|---|---|
| Total degassing ($v_i$–$v_s$) | 88 | 51 | 52 | 90 | 98 | 92 |
| Amount retained in solidified products ($v_s$) | 12 | 49 | 48 | 10 | 2 | 8 |
| Degassing at vents ($v_i$–$v_t$) | 71 | 27 | 29 | 70 | 82 | 74 |
| Degassing during lava transport ($v_t$–$v_l$) | 8 | 13 | 6 | – | – | – |
| Degassing after lava emplacement ($v_l$–$v_c$) | 9 | 11 | 17 | 20[b] | 16[b] | 18[b] |

[a] From Óskarsson et al. (1984) and Sigvaldason and Óskarsson (1986). Numbers in *italics* probably overestimate the $CO_2$ concentration in the Laki products and should be regarded as maximum values

[b] Calculated as the total amount released by the lava. See text for definitions and further discussion

**Table 7** Estimates on the mass (in megatons) of volatiles released by the Laki magma at various stages in the eruption

| | $SO_2$ | HCl | HF | $H_2O$ | $CO_2$ | Σ |
|---|---|---|---|---|---|---|
| Original mass ($m_r$) | 139.1 | 13.2 | 29.1 | 262.6 | *354.3* | 798.3 |
| Total mass released ($m_b$) | 122.1 | 6.8 | 15.1 | 235.4 | *348.6* | 728.0 |
| Mass retained in solidified products ($m_s$) | 17.0 | 6.4 | 14.0 | 27.2 | 5.7 | 70.3 |
| Mass released at vents ($m_r$–$m_v$) | 98.4 | 3.6 | 8.3 | 183.1 | 292.8 | 585.0 |
| Mass released during lava transport ($m_v$–$m_l$) | 11.6 | 1.7 | 1.8 | – | – | – |
| Mass released after lava emplacement ($m_l$–$m_c$) | 12.5 | 1.5 | 5.0 | 52.3[a] | 55.8[a] | 143.4[a] |

Total volume of magma used in the calculations of 15.1 $km^3$ (lava 14.7 $km^3$; tephra 0.4 $km^3$) is from Thordarson and Self (1993) and the assumed magma density of 2750 kg $m^{-3}$ is from Metrich et al. (1991). See text for definitions and further discussion. Numbers in *italics* probably overestimate the $CO_2$ mass released by the Laki eruption and should be regarded as an absolute maximum

[a] Calculated as the total amount released by the lava

the constant required to convert the pure element to the species assumed to be present in the magma (e.g., $SO_2$, HCl, and HF). As an example, the average inclusion concentration of sulfur, 1677 ppm (0.1677 wt.%), transforms into ~139 Mt of $SO_2$ carried from depth to the surface by the erupting magma (Fig. 14; Table 7).

The total mass of each volatile species ($m_{x,b}$) released by the eruption is taken as the difference between the inclusion value and the amount retained in the solidified eruption products ($m_{x,s}$), or:

$$m_{x,b} = m_{x,r} - m_{x,s} = (M_r v_{x,i}) - (v_{x,t} M_t + v_{x,c} M_l)$$

where Mt is the mass of tephra and other symbols are as defined previously. Application of this equation indicates that more than 85% of the $SO_2$ and $H_2O$ escaped from the magma during the eruption (Table 6) and that the total amounts released were ~139 Mt $SO_2$ and ~263 Mt $H_2O$ (Fig. 14; Table 7). Although the $CO_2$ values reported in Table 6 may be overestimates (see above), we include them in our calculations. The results

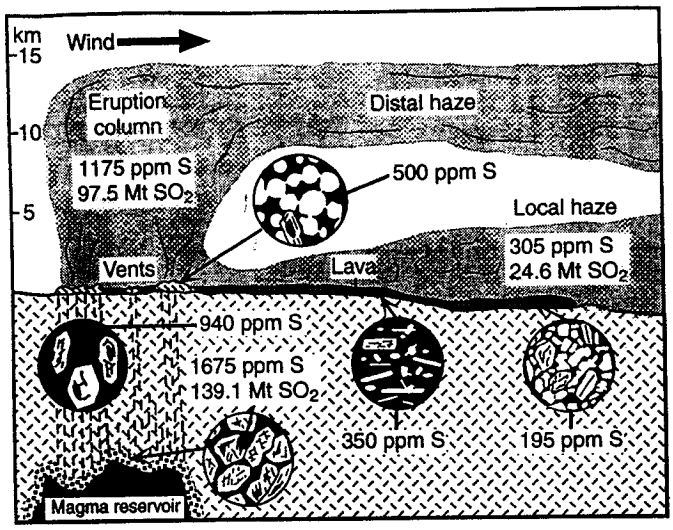


**Fig. 14** Illustration of the Laki eruption viewed from the southwest (not to scale) showing the amount of S retained in samples from various eruption stages and their relationship to the degassing of the magma. Also shown is the total amount of $SO_2$ dissolved in the Laki magma prior to eruption and the estimated $SO_2$ yield by various eruption stages. The gas columns and plumes generated by the magma degassing are shown as *fine stippled areas*. *Distal haze* denotes the gas liberated at the vents and carried to high altitudes by the eruption columns, and *local haze* denotes that produced by gas rising from the lava flow. Other features are as indicated in Fig. 4

imply that the Laki magma released a maximum of ~354 Mt $CO_2$ (Table 7). The fractions of HCl and HF released are considerably smaller, approximately 50% of the total mass originally dissolved in the magma. This implies that the mobility and solubility of Cl and F in the erupting liquid are governed by somewhat different chemical processes (Carroll and Webster 1994). The Laki eruption liberated a total of 6.8 and 15.1 Mt of HCl and HF, respectively. Our estimates suggest that the total volatile release by the eruption was ~730 Mt (Table 7).

The groundmass-glass sulfur concentrations in the phreatomagmatic tephra (mean 944±217 ppm) fall between that of the inclusions and the strombolian tephra. Furthermore, the estimated melt temperature of the phreatomagmatic tephra is near the reservoir temperature of the Laki magma (Fig. 12). This evidence suggests that the phreatomagmatic tephra was produced by early quenching and fragmentation of partly degassed magma within the conduit by explosive interaction of water and magma. The consistently lower, but uniform, S concentration of the strombolian tephra, however, implies that conduit degassing was near completion when fragmentation and venting occurred. The identical S, Cl, and F abundances in the strombolian tephra and proximal lava samples (Tables 4 and 5) support this conclusion. Approximately 70% of the total magmatic $SO_2$ and $H_2O$ was released as the magma emerged from the fissures (Table 6), and approximately 98 Mt $SO_2$ and 183 Mt $H_2O$ were discharged into the atmosphere above the Laki fissures at times of vigorous explosive activity (Fig. 14; Table 7). Moreover, taking the $CO_2$ concentrations in Table 6 at face value, the Laki magma released ~80% of its carbon dioxide (~293 Mt $CO_2$) through vent degassing. The vent degassing of HCl and HF was considerably less, 27 and 29%, respectively, of the total magmatic mass of these volatiles, signifying an upper tropospheric/lower stratospheric loading of the order of 3.6 Mt for Cl and 8.3 Mt for F.

Volatile concentrations of medial and distal lava, which are very uniform after being corrected for degree of crystallinity (Table A-2, Appendix II), can be taken as the fraction of volatiles retained in the magma upon emplacement in the medial and distal areas of the lava field. The difference in the concentration of the strombolian tephra and the lava selvages (Table 6) can be used to estimate the volatile mass released during lava emplacement (Fig. 13). Similarly, the difference between the concentration in lava selvages and crystalline lava denotes the mass released during cooling and crystallization of the lava after the flow had stopped its advance. According to these arguments ~11.6 Mt $SO_2$, ~1.7 Mt HCl, and ~1.8 Mt HF were liberated from the moving lava during transport from vents, followed by release of ~12.5 Mt $SO_2$, ~1.5 Mt HCl, and ~5.0 Mt HF during cooling and crystallization (Fig. 14; Table 7).

## Discussion

### Magma degassing and implications for eruption dynamics

The S concentrations in Laki glass inclusions are consistent with observed S–FeO solubility relations in submarine tholeiites (Wallace and Carmichael 1992; Mathez 1976), suggesting that the Laki magma was near sulfur saturation prior to the eruption (Fig. 15). Even though the analysis of Óskarsson et al. (1984) overestimates the $CO_2$ concentrations in Laki inclusions, the results show clearly that the melt was above its $CO_2$ saturation limit before it erupted (Metrich et al. 1991). Furthermore, the concentrations of other volatiles measured in Laki inclusions imply that the melt was undersaturated with $H_2O$, Cl, and F (Johnson et al. 1994; Carroll and Webster 1994). These data imply that magma over-pressurization induced by $CO_2$ saturation was responsible for the onset of the Laki eruption and suggest an early exsolution of volatiles (primarily $CO_2$) either in the reservoir or in the lowest part of the feeder dike(s).

The S content of the groundmass glass from Laki products reflects progressive magma degassing during its rise through the crust and after its emergence from the vents as tephra and lava (Fig. 15). The differences in the melt temperatures and composition of the tephra types can be reconciled if the phreatomagmatic tephra was quenched at greater conduit depths than the strombolian tephra. The abundance of highly vesicular clasts

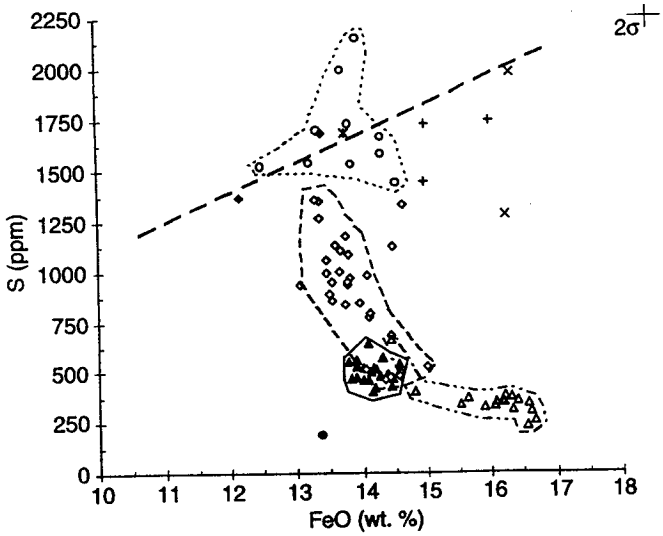


**Fig. 15** S (ppm) variation as a function of FeO (wt.%) in Laki samples. Note apparent negative correlation of S and FeO shown by phreatomagmatic tephra and strong clustering of strombolian tephra samples (see text for discussion). *Open circles* Laki-type inclusions; *asterisk* mean of Laki-type inclusions; *filled diamonds* inclusions with high MgO content; *pluses* inclusions with high FeO content; *crosses* inclusions with high FeO and $TiO_2$ content; *open diamonds* phreatomagmatic tephra; *filled triangles* strombolian tephra; *open triangles* lava selvages; *filled circle* mean of crystalline lava (whole rock). *Heavy broken line* indicates the sulfur solubility trend in submarine basalts as shown by Wallace and Carmichael (1992) and Mathez (1976)

in the phreatomagmatic tephra demonstrate that vesiculation and foam formation was well under way prior to the explosive interaction of water and magma which produced the deposits. Moreover, the data (Figs. 9b and 15) show that the magma had exsolved ~20–70 wt.% of its original S content when melt fragmentation and quenching occurred preventing further degassing. The more evolved composition (Fig. 7) and mature vesicle structure of the strombolian clasts (Fig. 8a) demonstrate that the strombolian tephra was produced by fragmentation of a foam layer, presumably at very shallow conduit levels. Cashman and Mangan (1994) have suggested that such magmatic foams are produced by "runaway" bubble nucleation and growth on timescales of hundreds of seconds, where vesiculation and magma fragmentation occur almost simultaneously. Episodic recurrence of this process may explain the relatively low, but uniform, S concentrations in all of the strombolian fall units (Fig. 15). The high abundances of Pele's hair in the strombolian tephra suggest that it was erupted by hot gas-rich fountains at high velocities (Thorarinsson 1984; Ólafsson et al. 1984; Shimozuru 1994), which may explain the fused outer surfaces of strombolian clasts (Fig. 8b). Furthermore, the analytical data imply that the lava contained ~500 ppm S when it flowed from the vents, or alternatively that the magma liberated ≥70 wt.% of its original S content through conduit and vent degassing. The results of Haughton et al. (1974) indicate that the sulfur capacity of the Laki magma at 1 atm pressure is 400 ppm, which is similar to the measured sulfur concentrations in strombolian tephra and the proximal lava, implying that the vent degassing of S was limited by its solubility.

The large fraction of volatiles released at the vents implies effective separation of volatiles and melt during ascent. In this context it is important to recognize that the Laki eruption was episodic, on the scale of several days to weeks, with intense fountaining and voluminous lava outpourings repeated each time a new pulse of magma reached the surface. Also note that the low ratio of tephra to lava volume (~1/35) shows that the bulk of the magma was erupted as lava. Estimated rise velocities of the magma pulses are in the range of 0.04–0.32 m/s (Thordarson 1990) and are similar to the advance velocities (0.03–0.08 m/s) of the lava surges produced by the eruption episodes (Thordarson and Self 1990). This suggests that the dominant lava emissions occurred at eruption velocities <1 m/s. Such low velocities imply an eruption in the homogeneous flow regime (gas and melt rise with the same velocity; Vergniolle and Jaupart 1986). However, the 800- to 1450-m-high fountains at Laki indicate magma exit velocities in the range of 130–170 m/s (Fig. 7b; Wilson and Head 1981), suggesting that the initial magmatic explosive phases of the episodes involved eruption velocities which were two orders of magnitude higher. Such intense fountains are driven by gas jets containing entrained melt fragments (Vergniolle and Jaupart 1986). Heights of fountains are controlled primarily by the contents of exsolved magmatic gas (Head and Wilson 1987). To produce the recorded fountain heights, the Laki magma had to have exsolved 50–75% of its original volatile content (Wilson and Head 1981). These considerations suggest that the explosive phases resulted from separated two-phase flow in the magma conduit, implying that transitions from separated to homogeneous flow regime occurred during each eruption episode (Vergniolle and Jaupart 1986).

As suggested above, the closed-cell spherical foam structure of the strombolian tephra is best explained by vesiculation and subsequent fragmentation at shallow conduit levels. However, this process alone cannot account for the high degree of vent degassing suggested by our data, because the volatile mass exsolved by the magma upon venting indicates a bulk gas-to-melt volume ratio of >100. As shown previously, the volume of a single fall unit is <3% of the total volume of magma erupted in separate episodes. Consequently, the cumulative bubble volume of the tephra can only be a fraction ($<<0.1$) of the total gas volume upon eruption, indicating that large quantities of gas exsolved from the melt without leaving clear physical evidence of its presence. These considerations suggest that most of the gas erupted as a free volatile phase, which supports the inferred evolution of separated conduit flow during the explosive phases. Thus, we conclude that the explosive phases at Laki involved an early and accelerated exso-

lution of volatiles (primarily $CO_2$), followed by a second vesiculation burst at shallow conduit levels which was caused by $H_2O$ and $SO_2$ oversaturation of the melt (Bottinga and Javoy 1991).

Based on the considerations of volatile degassing at Laki, the dynamics of the eruption may be viewed as follows: As the magma began its rise to the surface, volatile exsolution was accelerated, liberating initially mostly $CO_2$. Rapid coalescence of bubbles led to formation of a separated two-phase flow in the feeder dike which enhanced the driving-pressure gradient in the magma column (Vergniolle and Jaupart 1986), resulting in intense fountaining activity at the surface and efficient liberation of $CO_2$, $SO_2$, and $H_2O$. This initial bulk degassing resulted in a gradual, but rapid, transition from separated to homogeneous flow regime and deceleration of magma rise velocities. We speculate that during this transition period part of the magma became saturated with $H_2O$ and $SO_2$, triggering "runaway" vesiculation. These vesicles accumulated rapidly at the top of the magma column to form a gas-rich foam layer which disintegrated upon extrusion to produce the strombolian fall units. Trailing the foam head was more voluminous, less vesicular, partly degassed magma, corresponding to the lava-producing phase of the eruption episodes. Cyclic recurrence of these phenomena can explain the episodic nature of the eruption and the uniformity of the texture and clast morphology of the strombolian tephra deposits. The dominance of separated flow regimes at the beginning of each episode implies that the bulk of the volatiles were discharged during the vigorous explosive activity. The explosive phases also produced the highest eruption columns of the Laki eruption (Thordarson and Self 1993) and therefore are likely to have discharged large quantities of volatiles at or above the tropopause. Consequently, the effective altitude of atmospheric volatile-loading from eruptions such as Laki is best evaluated by the maximum height reached by the eruption columns.

## Fluorine and chlorine degassing

Many previous studies based on whole-rock analyses of crystalline lava and glassy tephra have argued that Cl and F are not effectively lost from the magma during an eruption (e.g., Sigvaldason and Óskarsson 1976, 1986; Aoki and Kanisawa 1979; Ishikawa et al. 1980; Aoki et al. 1981). These arguments are supported primarily by experimental Cl and F solubility data, theoretical and model considerations, and the relatively small variation in measured Cl and F concentrations ($\leq 20\%$) in samples representing various phases in a single eruption. However, Metrich (1990) and Metrich and Clocchiatti (1989) showed that the 1763 AD Etna magma lost 45% of its original Cl upon eruption. Results of Devine et al. (1984) indicate up to 50% Cl loss by magmas of intermediate compositions; similar results have been obtained from products of basaltic fissure eruptions in shallow marine and subaerial environments (Unni and Schilling 1978).

Our results show that the Laki magma liberated $\sim 50\%$ of its original Cl and F abundances during the eruption. Approximately half of the Cl and F released into the atmosphere was discharged at the Laki vents. The remainder was liberated during lava transport and during cooling of the lava after it was emplaced (Table 6). The nearly equal degrees of degassing for these two elements appear consistent with their similar chemical characteristics and expected compatibility at magmatic temperatures, especially in basaltic melts free of apatite and hydrous mineral phases (Carmichael et al. 1974). Laki inclusions have Cl and F contents which are well below HCl and HF saturation levels in basaltic melts (Caroll and Webster 1994); thus, fluxing by other effervescing volatiles is a likely explanation for the effective removal of these elements from the Laki magma (Iwasaki and Katsura 1967; Rowe and Schilling 1979). Similar analyses of products from other basaltic fissure eruptions in Iceland also indicate that approximately half of the magmatic Cl and F was released into the atmosphere upon extrusion (Thordarson 1995).

## Atmospheric loading of $SO_2$ and rate of degassing with time

In the case of short-lived explosive eruptions with well-documented atmospheric perturbations, such as El Chichón 1982 and Pinatubo 1991, the potential amount of $H_2SO_4$ aerosols generated from the measured $SO_2$ emission by the eruption is only slightly less than the maximum measured stratospheric aerosol loading (e.g., Hofmann 1987; McCormick et al. 1995). Obviously, this does not hold for predominantly effusive fissure eruptions, such as Laki, where the ratio of tephra to lava is less than 1:20 and the eruption columns just manage to penetrate the tropopause. In assessing the $SO_2$ loading of long-duration (months to years) lava-producing fissure eruptions, it is important to evaluate the dynamics of degassing, the timing, and the degree of degassing by separate eruptive phases and episodes. One must also consider the volume erupted by each phase and episode, changes in discharge, and eruptive behavior.

Contemporary descriptions of the Laki eruption indicate that the highest rates of atmospheric volatile mass loading (i.e., magma degassing) coincided with periods of vigorous eruption and peak magma discharge at the Laki fissures (Thordarson and Self 1993; Thordarson 1995), implying a direct correlation between magma and gas discharge. The Laki eruption produced $\sim 9.0\ km^3$ of lava and tephra in the first 40 days, approximately 60% of the total volume produced. Consequently, Laki released $\sim 73.0$ Mt of $SO_2$ into the atmosphere during this period, equivalent to atmospheric mass loading of $\sim 1.7$ Mt per day. With 70% of this amount liberated at the vents and carried by the eruption columns to altitudes between 6 and 13 km, the

Laki eruption is estimated to have injected ~1.3 Mt per day of $SO_2$ into the upper troposphere and the lower stratosphere during this period. For comparison, the annual $SO_2$ discharge by the present Pu'u'O'o–Kupaianaha eruption at Kilauea, Hawaii, is ~0.7 Mt (Elias et al. 1993) or approximately half of the *daily* output by the Laki fissures. The estimated $SO_2$ yield of the May to August 1783 Asama eruption in Japan is 1.0–3.5 Mt (Thordarson 1995), equivalent to the amount of $SO_2$ released by Laki in a few days.

The Laki eruption produced approximately 4.0 $km^3$ of lava and tephra between August and October, half the amount produced during the first 40 days of the eruption (Thordarson and Self 1993). Magma production at the Laki fissures in August and September of 1783 is estimated as 3.5 $km^3$ in 60 days (Thordarson 1990, 1991) yielding 0.5–0.6 Mt $SO_2$ emitted daily, dropping to ~0.2 Mt per day in October and less than 0.1 Mt per day during the waning stages of the eruption.

The moving Laki lava flow released approximately 25 Mt of $SO_2$ into the troposphere (Table 8), with an almost equal amount released by degassing of liquid lava during and after emplacement, consistent with contemporary descriptions of gases rising from the advancing lava and a 2-year postemplacement emission of steam and other gases (Steingrímsson 1783, 1788). The lava emissions represent approximately one fifth of the total $SO_2$ released by the Laki eruption.

A total atmospheric $SO_2$ loading of ~122 Mt by the Laki event gives a potential $H_2SO_4$-aerosol yield of ~250 Mt. Assuming that the aerosol particles consisted of 75% $H_2SO_4$ and 25% $H_2O$ (Thomason and Osborn 1992), this is equivalent to ~185 Mt of pure $H_2SO_4$. According to the degassing rates given above, the eruption released sufficient mass of $SO_2$ in the first 2 months to generate ~175 Mt of $H_2SO_4$. This value is similar to an independent estimate of ~200 Mt (Stothers 1996) for the accumulative total column $H_2SO_4$-aerosol yield from Laki in the same period using information on atmospheric turbidity over Europe. The agreement of two totally different methods of estimating the atmospheric loading indicates that the petrologic method gives reliable results for Laki. These values cannot be directly compared with earlier aerosol mass estimates based on the amount of Laki sulfate fallout in Greenland (e.g., Clausen and Hammer 1988), because the findings of Fiacco et al. (1994) indicate that the fallout represents only the portion of the Laki aerosol cloud which remained aloft in the atmosphere for more than 1 year. The volatile contribution due to degassing of the Laki lava flow is only 18% of the total amount released by the magma. These gaseous emissions were confined mostly to the lowest regions of the troposphere and therefore only important on a regional scale in Iceland. A more comprehensive discussion on the environmental and climatic effects of the Laki eruption is presented by Fiacco et al. (1994) and Thordarson, 1995.

## Appendix I

Sample locations and representation

Systematic sampling of vent and rootless-cone tephra, and lava, was conducted to obtain an even spatial and temporal coverage of the eruption products (Figs. 1 and 4; see also Table 1). The phreatomagmatic tephra and the strombolian tephra samples (Table 1) provide information about the volatile and magma composition during magma rise in the conduit and upon vent extrusion. The groundmass glass of lava selvages and rootless-cone tephra represent the liquid lava which was quenched rapidly upon emplacement at the respective sample location. These samples provide information about the chemical and the physical properties of the liquid lava at various distances from source. Samples VRC-9, VRC-11, L-23, and LEIRC-3–1 to LEIRC-20A-8 represent the lava stream which emerged from the fissure segments SW of Laki and advanced down the Sída highlands through the Hellisá river valley before entering the Skaftár River gorge (Thordarson and Self 1993). VRC-9 and VRC-11 are tephra samples from rootless cones located ~2 km south of the fissures in Varmárdalur (location 9) and sample L-23 is from the basal selvage of lava flow unit near Kálfá (location 7) and field relations suggest that both units were formed before 30 June 1783 (Thordarson 1990, 1991). The lava and tephra samples from the Leidólfsfell rootless cone group (location 12) were produced by explosive interaction of lava and water around 17 June 1783 (Steingrímsson 1783, 1788; Thordarson 1990, 1991). Sample locations 7 and 12 are 16 and 21 km from the source, respectively, and thus come from the medial part of the early formed lavas. The distal lava of the same flow field is represented by samples L-24 and L-25, which compose the basal and surface selvage, respectively, of a single 3.5- to 6.0-m-thick flow unit (Sal-9) at Eldvatnsbrú (location 8). This flow unit was emplaced sometime between 14 June and 12 July 1783. The samples L-20, L-21 (location 6), BRC-9 (location 10), and NIRC-7 (location 11) are from flow units which belong to the lavas produced by the fissures NE of Laki between 1 August and 1 October. At location 6, a distance of 14 km from source, the Laki lava is composed of two emplacement units (E1 and E2), each containing several flow units. Sample L-20 is from the surface glass selvage of the uppermost flow unit of the lower emplacement unit (E1FU4), whereas L-21 is the basal selvage of a flow lobe within the lower half of the upper emplacement unit (E2FU2). Sample BRC-9 is tephra from the Blængur rootless cone group, located 0.5 km south of fissures northeast of Laki and sample NIRC-7 is tephra from the Innrieyrar rootless cone group located 1.5 km north of the fissures. Both samples are representative of the proximal lava.

## Appendix II

**Table AII-1** Major element and volatile composition of the samples used in this study

Laki inclusions:

| Label | $SiO_2$ | $TiO_2$ | $Al_2O_3$ | FeO | MnO | MgO | CaO | $Na_2O$ | $K_2O$ | $P_2O_5$ | Sum | S | Cl | F | Mg# | *N* | Host |
|---|---|---|---|---|---|---|---|---|---|---|---|---|---|---|---|---|---|
| *Group 1. Laki composition* | | | | | | | | | | | | | | | | | |
| L-i-1 | 49.88 | 2.87 | 12.73 | 14.55 | 0.24 | 6.05 | 10.14 | 2.69 | 0.47 | 0.19 | 99.82 | 1430 | 270 | 660 | 42.55 | 1 | P |
| L-i-2 | 49.61 | 2.93 | 12.06 | 13.74 | 0.22 | 6.31 | 10.00 | 2.91 | 0.53 | 0.34 | 98.65 | 1985 | 250 | 820 | 44.98 | 1/2 | P |
| L-i-3 | 49.61 | 2.85 | 13.07 | 13.88 | 0.24 | 5.77 | 10.39 | 3.01 | 0.42 | 0.25 | 99.50 | 1520 | 300 | 705 | 42.56 | 6/5 | P |
| L-i-4 | 49.72 | 2.88 | 12.50 | 14.33 | 0.23 | 5.91 | 10.51 | 2.85 | 0.41 | 0.30 | 99.65 | 1570 | 290 | 530 | 42.35 | 4/3 | P |
| L-i-5 | 49.25 | 2.93 | 13.40 | 13.98 | 0.24 | 5.78 | 10.25 | 2.98 | 0.42 | 0.27 | 99.50 | 2140 | 290 | 665 | 42.40 | 2/3 | P |
| L-i-6 | 49.83 | 2.73 | 13.56 | 13.24 | 0.17 | 5.91 | 10.49 | 2.85 | 0.38 | 0.33 | 99.50 | 1530 | 360 | 720 | 44.28 | 1 | O |
| L-i-7 | 49.24 | 3.07 | 13.17 | 14.33 | 0.25 | 5.57 | 10.38 | 2.83 | 0.47 | 0.31 | 99.62 | 1660 | 270 | 530 | 40.92 | 2/3 | O |
| L-i-8 | 49.48 | 3.21 | 13.41 | 13.84 | 0.18 | 5.32 | 10.68 | 2.74 | 0.36 | 0.24 | 99.46 | 1720 | 440 | 690 | 40.63 | 2 | O |
| L-i-9 | 49.69 | 3.25 | 13.29 | 13.35 | 0.19 | 5.83 | 10.66 | 2.85 | 0.36 | 0.24 | 99.72 | 1690 | 350 | 550 | 43.77 | 1 | O |
| L-i-10 | 50.51 | 2.84 | 13.36 | 12.51 | 0.22 | 5.35 | 10.98 | 2.64 | 0.38 | 0.31 | 99.10 | 1515 | 270 | 780 | 43.24 | 1/2 | C |
| *Group 2. High FeO* | | | | | | | | | | | | | | | | | |
| L-i-11 | 48.70 | 3.00 | 12.48 | 16.01 | 0.24 | 5.51 | 10.25 | 2.46 | 0.39 | 0.34 | 99.39 | 1740 | 185 | 450 | 38.02 | 2 | O |
| L-i-12 | 49.05 | 2.98 | 12.01 | 15.00 | 0.23 | 6.38 | 10.60 | 2.43 | 0.57 | 0.26 | 99.51 | 1720 | 260 | 530 | 43.12 | 2 | O |
| L-i-13 | 50.05 | 3.10 | 11.74 | 14.99 | 0.23 | 5.99 | 10.38 | 2.41 | 0.48 | 0.32 | 99.69 | 1435 | 295 | 630 | 41.61 | 2 | P |
| *Group 3. High FeO and $TiO_2$* | | | | | | | | | | | | | | | | | |
| L-i-14 | 48.86 | 3.40 | 13.15 | 16.36 | 0.24 | 4.78 | 9.61 | 2.58 | 0.42 | 0.33 | 99.73 | 1970 | 310 | 710 | 34.23 | 2/3 | P |
| L-i-15 | 48.87 | 3.45 | 13.00- | 16.26 | 0.19 | 4.62 | 9.50 | 2.55 | 0.48 | 0.37 | 99.29 | 1275 | 285 | 610 | 33.61 | 4/3 | P |
| *Group 4. High MgO* | | | | | | | | | | | | | | | | | |
| L-i-16 | 49.65 | 2.17 | 13.45 | 12.17 | 0.21 | 6.96 | 11.51 | 3.01 | 0.38 | 0.20 | 99.72 | 1244 | 262 | 618 | 50.44 | 4/5 | P |
| L-i-17 | 49.13 | 2.00 | 12.03 | 13.41 | 0.23 | 8.47 | 11.37 | 2.47 | 0.39 | 0.17 | 99.67 | 1675 | 198 | 562 | 52.95 | 4/5 | P |

Strombolian tephra:

| Label | $SiO_2$ | $TiO_2$ | $Al_2O_3$ | FeO | MnO | MgO | CaO | $Na_2O$ | $K_2O$ | $P_2O_5$ | Sum | S | Cl | F | Mg# | Ves.% | Cr.% | *N* |
|---|---|---|---|---|---|---|---|---|---|---|---|---|---|---|---|---|---|---|
| LS1-01-11 | 49.97 | 3.05 | 13.24 | 14.19 | 0.23 | 5.41 | 10.08 | 2.81 | 0.45 | 0.35 | 99.78 | 418 | 150 | 468 | 40.43 | 65 | 1 | 3 |
| LS1-01-12 | 50.13 | 3.01 | 13.28 | 14.15 | 0.22 | 5.43 | 10.14 | 2.69 | 0.49 | 0.36 | 99.90 | 402 | 159 | 431 | 40.62 | 45 | 1 | 3 |
| LS1-04-12 | 50.09 | 3.08 | 13.21 | 14.27 | 0.21 | 5.47 | 9.83 | 2.83 | 0.45 | 0.32 | 99.75 | 480 | 225 | 515 | 40.57 | 50 | 3 | 12/9 |
| LS1-04-14 | 50.11 | 3.10 | 13.24 | 14.49 | 0.19 | 5.37 | 9.87 | 2.75 | 0.46 | 0.35 | 99.92 | | | | 39.78 | 70 | 2 | 3 |
| LS1-04-17 | 49.98 | 3.04 | 13.19 | 14.45 | 0.21 | 5.47 | 9.77 | 2.79 | 0.45 | 0.28 | 99.63 | 425 | 235 | 445 | 40.26 | 75 | 1 | 4 |
| LS1-04-18 | 50.01 | 3.06 | 13.18 | 14.36 | 0.22 | 5.37 | 9.75 | 2.85 | 0.44 | 0.32 | 99.55 | 480 | 225 | 500 | 39.98 | 88 | 1 | 4 |
| LS2-06-11 | 49.96 | 3.01 | 13.38 | 14.12 | 0.24 | 5.44 | 10.15 | 2.83 | 0.46 | 0.35 | 99.92 | 498 | 148 | 455 | 40.70 | 55 | 5 | 3 |
| LS2-06-12 | 49.93 | 3.08 | 13.20 | 14.56 | 0.26 | 5.31 | 9.87 | 2.80 | 0.49 | 0.36 | 99.86 | 534 | 147 | 518 | 39.41 | 55 | 3 | 3/2 |
| LS3-02-31 | 49.96 | 3.01 | 13.24 | 14.00 | 0.21 | 5.42 | 9.90 | 2.84 | 0.45 | 0.31 | 99.34 | 455 | 245 | 445 | 40.81 | 71 | 1 | 3/4 |
| LS3-02-32 | 49.92 | 3.02 | 13.20 | 14.17 | 0.21 | 5.44 | 9.81 | 2.82 | 0.44 | 0.26 | 99.29 | 515 | 245 | 525 | 40.64 | 84 | 1 | 3/4 |
| LS3-02-33 | 49.93 | 3.01 | 13.21 | 13.92 | 0.21 | 5.37 | 9.89 | 2.71 | 0.46 | 0.34 | 99.05 | 470 | 245 | 525 | 40.75 | 78 | 1 | 3 |
| LS3-02-34 | 49.82 | 3.02 | 13.22 | 13.84 | 0.23 | 5.45 | 9.86 | 2.59 | 0.44 | 0.33 | 98.79 | 465 | 245 | 450 | 41.24 | 82 | 1 | 3 |
| LS3-02-21 | 49.98 | 3.04 | 13.18 | 13.92 | 0.22 | 5.39 | 9.89 | 2.56 | 0.44 | 0.27 | 98.90 | 520 | 320 | 530 | 40.83 | 84 | 1 | 3 |
| LS3-02-22 | 49.61 | 3.00 | 13.12 | 14.08 | 0.20 | 5.44 | 9.92 | 2.75 | 0.47 | 0.28 | 98.87 | 640 | 250 | 310 | 40.78 | 90 | 0 | 3 |
| LS3-02-23 | 50.18 | 3.04 | 13.31 | 13.79 | 0.22 | 5.43 | 9.85 | 2.53 | 0.46 | 0.32 | 99.12 | 545 | 280 | 485 | 41.22 | 77 | 0 | 3 |
| LS3-02-24 | 49.20 | 2.94 | 13.19 | 13.92 | 0.23 | 5.37 | 9.77 | 2.67 | 0.44 | 0.34 | 98.07 | 555 | 175 | 415 | 40.76 | 88 | 0 | 3 |
| LS3-03-11 | 49.92 | 2.96 | 13.15 | 14.00 | 0.19 | 5.43 | 9.92 | 2.86 | 0.43 | 0.30 | 99.15 | 515 | 315 | 450 | 40.88 | 78 | 1 | 3 |
| LS3-03-12 | 49.85 | 3.04 | 13.08 | 14.20 | 0.24 | 5.33 | 9.88 | 2.80 | 0.44 | 0.27 | 99.14 | 510 | 320 | 525 | 40.09 | 57 | 1 | 3/4 |
| LS3-03-13 | 49.84 | 3.04 | 13.28 | 14.30 | 0.19 | 5.44 | 9.91 | 2.63 | 0.47 | 0.32 | 99.41 | 570 | 200 | 485 | 40.40 | 61 | 1 | 3/4 |
| LS3-03-15 | 49.23 | 3.03 | 13.14 | 14.08 | 0.21 | 5.43 | 9.77 | 2.71 | 0.42 | 0.26 | 98.28 | 455 | 250 | 510 | 40.73 | 72 | 1 | 3 |
| LS4-01-11 | 50.10 | 3.12 | 13.11 | 14.38 | 0.23 | 5.20 | 10.12 | 2.80 | 0.49 | 0.36 | 99.92 | 484 | 164 | 496 | 39.19 | 45 | 5 | 3 |
| LS4-01-12 | 50.03 | 3.15 | 13.06 | 14.46 | 0.25 | 5.22 | 10.08 | 2.85 | 0.48 | 0.36 | 99.94 | 461 | 134 | 482 | 39.14 | 48 | 2 | 3 |

Phreatomagmatic tephra:

| Label | $SiO_2$ | $TiO_2$ | $Al_2O_3$ | FeO | MnO | MgO | CaO | $Na_2O$ | $K_2O$ | $P_2O_5$ | Sum | S | Cl | F | Mg# | Ves.% | Cr.% | *N* |
|---|---|---|---|---|---|---|---|---|---|---|---|---|---|---|---|---|---|---|
| LP1-U2-1 | 49.67 | 2.80 | 13.38 | 13.69 | 0.22 | 5.85 | 11.02 | 2.23 | 0.62 | 0.25 | 99.73 | 1090 | 256 | 345 | 43.19 | 2 | 5 | 7/8 |
| LP1-U2-2 | 49.50 | 2.74 | 13.50 | 13.47 | 0.21 | 5.98 | 11.07 | 2.34 | 0.49 | 0.24 | 99.54 | 1050 | 190 | 415 | 44.18 | 0 | 1 | 5/6 |
| LP1-U2-3 | 49.88 | 2.77 | 13.45 | 13.37 | 0.18 | 5.88 | 11.20 | 2.28 | 0.55 | 0.26 | 99.81 | 1115 | 210 | 460 | 43.93 | 0 | 1 | 2/3 |
| LP1-U2-4 | 49.67 | 2.74 | 13.32 | 13.68 | 0.21 | 5.75 | 10.96 | 2.32 | 0.55 | 0.25 | 99.46 | 995 | 200 | 455 | 42.82 | 1 | 2 | 3/4 |
| LP1-U2-21 | 49.52 | 2.72 | 13.25 | 13.79 | 0.17 | 6.01 | 11.02 | 2.21 | 0.71 | 0.23 | 99.63 | 930 | 180 | 460 | 43.71 | 54 | 5 | 2/4 |
| LP1-U2-61 | 50.19 | 3.10 | 13.17 | 14.58 | 0.25 | 5.26 | 9.65 | 2.30 | 0.71 | 0.25 | 99.47 | 490 | 130 | 335 | 39.14 | 55 | 2 | 1/3 |
| LP1-U2-62 | 49.53 | 2.98 | 13.25 | 14.56 | 0.23 | 5.64 | 10.12 | 2.45 | 0.72 | 0.33 | 99.81 | 1260 | 240 | 265 | 40.85 | 10 | 1 | 2 |
| LP1-U3-2 | 49.61 | 2.84 | 13.46 | 13.61 | 0.23 | 5.71 | 11.12 | 2.41 | 0.46 | 0.28 | 99.71 | 1125 | 185 | 485 | 42.77 | 49 | 7 | 2/4 |
| LP1-U5-22 | 49.34 | 2.69 | 13.40 | 13.82 | 0.22 | 5.93 | 10.95 | 2.41 | 0.69 | 0.24 | 99.68 | 1075 | 450 | 320 | 43.34 | 38 | 1 | 2 |
| LP1-U5-42 | 49.71 | 3.08 | 13.22 | 13.97 | 0.23 | 5.33 | 9.74 | 2.74 | 0.44 | 0.29 | 98.76 | 835 | 240 | 485 | 40.48 | 50 | 10 | 2/3 |
| LP1-U5-61 | 49.76 | 3.01 | 13.23 | 14.11 | 0.22 | 5.35 | 9.92 | 2.76 | 0.45 | 0.31 | 99.13 | 770 | 295 | 460 | 40.32 | 69 | 1 | 2 |
| LP1-U5-62 | 49.98 | 3.05 | 13.06 | 14.12 | 0.21 | 5.33 | 9.80 | 2.82 | 0.44 | 0.30 | 99.09 | 785 | 350 | 440 | 40.21 | 59 | 1 | 2 |
| LP2-05-11 | 49.90 | 3.00 | 13.46 | 13.91 | 0.23 | 5.25 | 10.14 | 2.86 | 0.47 | 0.35 | 99.58 | 958 | 143 | 426 | 40.21 | 28 | 1 | 3 |
| LP2-05-12 | 49.52 | 2.38 | 13.70 | 12.60 | 0.21 | 6.46 | 11.70 | 2.58 | 0.32 | 0.25 | 99.71 | 980 | 122 | 381 | 47.75 | 0 | 1 | 2 |
| LP2-05-13 | 50.10 | 2.96 | 13.27 | 14.27 | 0.23 | 5.40 | 10.21 | 2.89 | 0.46 | 0.33 | 100.12 | 507 | 137 | 505 | 40.25 | 80 | 2 | 3/1 |

*(Continued)*

**Table AII-1** (Continued)

Lava selvages:

| Label | $SiO_2$ | $TiO_2$ | $Al_2O_3$ | FeO | MnO | MgO | CaO | $Na_2O$ | $K_2O$ | $P_2O_5$ | Sum | S | Cl | F | Mg# | Cr.% | *N* | D (km) |
|---|---|---|---|---|---|---|---|---|---|---|---|---|---|---|---|---|---|---|
| L-20 | 49.75 | 3.78 | 11.79 | 16.31 | 0.27 | 4.52 | 9.37 | 2.78 | 0.56 | 0.43 | 99.55 | 460 | 270 | 613 | 33.07 | 35 | 16/11 | 14 |
| L-21 | 50.03 | 3.86 | 11.84 | 16.05 | 0.25 | 4.66 | 9.48 | 2.78 | 0.57 | 0.36 | 99.89 | 434 | 309 | 608 | 34.10 | 23 | 75/39 | 14 |
| L-23 | 50.31 | 3.64 | 11.49 | 16.57 | 0.26 | 4.77 | 8.81 | 2.56 | 0.90 | 0.37 | 99.69 | 442 | 228 | 521 | 33.88 | 30 | 3/3 | 16 |
| L-24 | 49.78 | 3.80 | 11.85 | 16.17 | 0.27 | 4.69 | 9.43 | 2.66 | 0.55 | 0.36 | 99.56 | 467 | 217 | 604 | 34.05 | 38 | 4/16 | 45 |
| L-25 | 49.78 | 3.82 | 11.77 | 16.20 | 0.29 | 4.69 | 9.29 | 2.75 | 0.54 | 0.39 | 99.51 | 470 | 226 | 594 | 34.01 | 35 | 5/3 | 45 |

Rootless cone tephra RCT-groundmass glass:

| Label | $SiO_2$ | $TiO_2$ | $Al_2O_3$ | FeO | MnO | MgO | CaO | $Na_2O$ | $K_2O$ | $P_2O_5$ | Sum | S | Cl | F | Mg# | Cr.% | *N* | D (km) |
|---|---|---|---|---|---|---|---|---|---|---|---|---|---|---|---|---|---|---|
| VRC-9-1 | 49.89 | 3.48 | 12.12 | 15.52 | 0.25 | 4.80 | 10.00 | 2.77 | 0.53 | 0.39 | 99.76 | 451 | 182 | 496 | 35.53 | 35 | 3/3 | 2 |
| VRC-11-11 | 49.66 | 3.68 | 11.98 | 15.90 | 0.24 | 4.67 | 9.90 | 2.82 | 0.56 | 0.42 | 99.83 | 435 | 168 | 471 | 34.35 | 35 | 3/2 | 2 |
| VRC-11-12 | 49.95 | 3.67 | 12.00 | 16.08 | 0.26 | 4.59 | 9.79 | 2.80 | 0.57 | 0.42 | 100.12 | 447 | 165 | 644 | 33.70 | 28 | 3/3 | 2 |
| BRC-9-31 | 50.06 | 3.15 | 13.28 | 14.45 | 0.19 | 5.25 | 9.88 | 2.77 | 0.44 | 0.36 | 99.84 | 740 | 270 | 465 | 39.32 | 12 | 4/4 | 0.5 |
| BRC-9-32 | 48.81 | 4.37 | 13.04 | 14.81 | 0.22 | 4.78 | 9.70 | 2.61 | 0.79 | 0.73 | 99.87 | 459 | 268 | 397 | 37.31 | 15 | 3/3 | 0.5 |
| BRC-5-1 | 48.91 | 3.39 | 12.05 | 16.92 | 0.27 | 4.76 | 10.09 | 2.66 | 0.43 | 0.37 | 99.86 | 914 | 120 | 454 | 33.37 | 2 | 3/3 | 0.5 |
| NIRC-7-11 | 49.62 | 3.60 | 11.97 | 15.64 | 0.25 | 4.65 | 10.12 | 2.84 | 0.62 | 0.42 | 99.74 | 435 | 201 | 482 | 34.62 | 18 | 2/3 | 1.5 |
| NIRC-7-12 | 49.87 | 3.71 | 11.90 | 16.22 | 0.26 | 4.63 | 9.65 | 2.21 | 0.78 | 0.41 | 99.62 | 448 | 173 | 534 | 33.70 | 18 | 2/3 | 1.5 |
| LEIRC-3-1 | 49.54 | 3.86 | 11.69 | 16.56 | 0.27 | 4.64 | 9.37 | 2.75 | 0.58 | 0.44 | 99.72 | 335 | 190 | 575 | 33.31 | 45 | 8/5 | 21 |
| LEIRC-3-2 | 49.67 | 3.94 | 11.71 | 16.61 | 0.25 | 4.59 | 9.33 | 2.75 | 0.56 | 0.48 | 99.87 | 435 | 250 | 535 | 32.97 | 45 | 8/5 | 21 |
| LEIRC-3A-1 | 49.48 | 4.34 | 11.45 | 17.69 | 0.24 | 4.10 | 9.03 | 2.59 | 0.65 | 0.62 | 100.18 | | | | 29.22 | 50 | 4 | 21 |
| LEIRC-41-3 | 49.86 | 3.91 | 11.81 | 16.26 | 0.20 | 4.79 | 9.50 | 2.69 | 0.53 | 0.46 | 100.02 | | | | 34.40 | 30 | 3 | 21 |
| LEIRC-42-3 | 49.71 | 3.92 | 11.54 | 16.67 | 0.25 | 4.51 | 9.19 | 2.81 | 0.57 | 0.40 | 99.57 | 340 | 215 | 540 | 32.54 | 30 | 5/5 | 21 |
| LEIRC-20A-8 | 49.86 | 3.88 | 11.75 | 16.34 | 0.22 | 4.63 | 9.36 | 2.76 | 0.56 | 0.39 | 99.76 | 405 | 265 | 495 | 33.55 | 30 | 5/5 | 21 |

RCT whole-rock composition:

| Label | $SiO_2$ | $TiO_2$ | $Al_2O_3$ | FeO | MnO | MgO | CaO | $Na_2O$ | $K_2O$ | $P_2O_5$ | Sum | Mg# | D (km) |
|---|---|---|---|---|---|---|---|---|---|---|---|---|---|
| LEIRC-02 | 49.60 | 2.74 | 13.31 | 14.03 | 0.22 | 5.92 | 10.46 | 2.67 | 0.51 | 0.41 | 99.87 | 42.91 | 21 |
| LEIRC-03A | 49.59 | 2.66 | 13.36 | 13.66 | 0.24 | 6.08 | 10.60 | 2.74 | 0.53 | 0.41 | 99.87 | 44.23 | 21 |
| LEIRC-12 | 49.07 | 2.80 | 13.52 | 13.96 | 0.23 | 5.85 | 10.87 | 2.65 | 0.50 | 0.42 | 99.85 | 42.75 | 21 |

New whole-rock analyses of Laki lava:

| Label | $SiO_2$ | $TiO_2$ | $Al_2O_3$ | FeO | MnO | MgO | CaO | $Na_2O$ | $K_2O$ | $P_2O_5$ | Sum | Mg# | D (km) |
|---|---|---|---|---|---|---|---|---|---|---|---|---|---|
| L-3 | 50.04 | 2.77 | 13.88 | 13.73 | 0.22 | 5.55 | 10.42 | 2.45 | 0.42 | 0.28 | 99.76 | 41.88 | 1 |
| L-9 | 50.10 | 2.74 | 13.86 | 13.97 | 0.22 | 5.49 | 10.43 | 2.39 | 0.43 | 0.29 | 99.92 | 41.21 | 1 |
| LEI-04 | 49.58 | 2.71 | 13.27 | 13.98 | 0.23 | 5.93 | 10.41 | 2.81 | 0.54 | 0.41 | 99.87 | 43.04 | 21 |
| LEI-12 | 50.05 | 2.66 | 13.49 | 13.33 | 0.22 | 5.88 | 10.68 | 2.61 | 0.51 | 0.44 | 99.85 | 44.01 | 21 |
| L-14 | 50.17 | 2.80 | 13.96 | 13.96 | 0.22 | 5.52 | 10.42 | 2.42 | 0.41 | 0.29 | 100.17 | 41.35 | 47 |

Host, mineral hosting inclusion; P, plagioclase; O, olivine; C, clinopyroxene; D, distance from vents in km; Mg# = 100 Mg/(Mg+Fe*), Fe* = total Fe; Ves.% and Cr.%, vesicularity and crystallinity respectively; *N*, number of analyses

**Table AII-2** Correction of measured S, Cl and F values in Laki lava selvages and rootless cone tephras for the effect of crystallization during lava emplacement

| Label | Mg# | FeO | Cr.% | S | S[a] | Cl | Cl[a] | F | F[a] | *N* |
|---|---|---|---|---|---|---|---|---|---|---|
| **Lava selvage** | | | | | | | | | | |
| L-20 | 33.07 | 16.31 | 32 | 460 | 375 | 270 | 220 | 615 | 500 | 11 |
| L-21 | 34.10 | 16.05 | 23 | 435 | 330 | 310 | 235 | 610 | 460 | 39 |
| L-23 | 32.73 | 16.42 | 30 | 440 | 340 | 230 | 175 | 520 | 400 | 6 |
| L-24 | 34.05 | 16.17 | 38 | 490 | 355 | 195 | 145 | 545 | 395 | 16 |
| L-25 | 34.01 | 16.17 | 35 | 470 | 350 | 225 | 165 | 595 | 440 | 3 |
| **Rootless cone tephra** | | | | | | | | | | |
| VRC-9-1 | 35.53 | 15.52 | 35 | 451 | 334 | 182 | 135 | 496 | 367 | 3 |
| VRC-11-11 | 34.35 | 15.90 | 35 | 435 | 322 | 168 | 124 | 471 | 349 | 3 |
| VRC-11-12 | 33.70 | 16.08 | 28 | 447 | 349 | 165 | 129 | 644 | 503 | 3 |
| BRC-9-31 | 39.32 | 14.45 | 12 | 740 | 660 | 270 | 240 | 465 | 415 | 3 |
| BRC-9-32 | 37.31 | 14.81 | 15 | 459 | 400 | 265 | 230 | 395 | 345 | 3 |
| BRC-5-1 | 33.37 | 16.92 | 2 | 914 | 896 | 120 | 117 | 454 | 445 | 3 |
| NIRC-7-11 | 34.62 | 15.64 | 18 | 435 | 368 | 201 | 171 | 482 | 408 | 3 |
| NIRC-7-12 | 33.70 | 16.22 | 18 | 448 | 380 | 173 | 147 | 534 | 452 | 3 |
| LEIRC-3-1 | 33.31 | 16.56 | 45 | 335 | 230 | 190 | 130 | 575 | 395 | 8/5 |
| LEIRC-3-2 | 32.97 | 16.61 | 45 | 435 | 300 | 250 | 170 | 535 | 370 | 8/5 |
| LEIRC-42-3 | 32.54 | 16.67 | 30 | 340 | 260 | 215 | 165 | 540 | 415 | 5/5 |
| LEIRC-20A-8 | 33.55 | 16.34 | 30 | 405 | 310 | 265 | 205 | 495 | 380 | 5/5 |

[a] Corrected values; *N*, number of analyses

**Acknowledgements** Support for this work was provided by the NASA Global Change Student Fellowship Fund, the National Science Foundation grant no. EAR-9118755, and NASA grants NAG5-1839 and NAGW-3721. Thanks are extended to Sara Finnemore for assistance with analysing mineral modes. We also thank Martha Sykes and John Mahoney, who read a previous version of the manuscript and made many useful suggestions. The manuscript was improved greatly by constructive reviews from Peter Michael, an anonymous reviewer, and Bruce F. Houghton. We thank Jocelyn McPhie for helpful editorial comments. Th. Thordarson also thanks the University of Hawaii at Manoa for support during completion of the PhD dissertation.

## References

Angell JK, Korshover J (1985) Surface temperature changes following the six major volcanic episodes between 1780–1980. J Clim Appl Meteor 24:937–951

Aoki K, Kanisawa S (1979) Fluorine contents of some hydrous minerals derived from upper mantle and lower crust. Lithos 12:167–171

Aoki K, Ishikawa K, Kanisawa S (1981) Fluorine geochemistry of basaltic rocks from continental and oceanic regions and petrogenetic application. Contrib Mineral Petrol 76:53–59

Bell JD, Humphries DJ (1972) Lakagígar fissure eruption. Progress in experimental petrology, publication series D2, pp 110–112

Bottinga Y, Javoy M (1991) The degassing of Hawaiian tholeiite. Bull Volcanol 53:73–85

Carmichael ISE, Turner FJ, Verhoogen J (1974) Igneous petrology. McGraw-Hill, New York

Carroll MR, Webster JD (1994) Solubilities of sulfur, noble gases, nitrogen, chlorine, and fluorine in magmas. Rev Mineral 30:231–271

Cashman KV, Mangan MT (1994) Physical aspects of magmatic degassing II. Constraints on vesiculation processes from textural studies of eruption products. Rev Mineral 30:447–478

Clausen HB, Hammer CU (1988) The Laki and Tambora eruptions as revealed in the Greenland ice cores from 11 locations. Ann Glaciol 10:16–22

Devine JD, Sigurdsson H, Davis AN, Self S (1984) Estimates of sulfur and chlorine yield to the atmosphere from volcanic eruptions and potential climatic effects. J Geophys Res 89:6309–6325

Dixon JE, Clague DA, Stolper EM (1991) Degassing of water, sulfur, and carbon in submarine lavas from Kilauea volcano, Hawaii. J Geol 99:371–394

Elias T, Sutton AJ, Stokes JB (1993) Current $SO_2$ emissions at Kilauea volcano: quantifying scattered degassing sources. EOS 74:670–671

Fiacco RJ Jr, Thordarson Th, Germani MS, Self S, Palais JM, Withlow S, Grootes PM (1994) Atmospheric aerosol loading and transport interpreted from ash particles and acidity due to the 1783–1784 Laki eruption in the GISP2 ice core. Quaternary Res 42:231–240

Gerlach TM, Westrich HR, Casadevall TJ, Finnegan DL (1994) Vapor saturation and accumulation in magmas of the 1989–1990 eruption of Redoubt volcano, Alaska. J Volcanol Geotherm Res 62:317–338

Grönvold K (1984) The petrochemistry of the Laki lava flow. In Einarsson T, Gudbergsson GM, Gunnlaugsson GA, Rafnsson S, Thorarinsson S (eds) Skaftáreldar 1783–1784:Ritgerdir og Heimildir. Mál og Menning, Reykjavík, pp 49–58

Haughton DR, Roeder PL, Skinner BJ (1974) Solubility of sulfur in mafic magmas. Econ Geol 69:451–467

Head JW, Wilson L (1987) Lava fountain heights at Pu'u'O'o, Kilauea, Hawaii: indicators of the amount and variation of exsolved magma volatiles. J Geophys Res 92:13715–13719

Helz RT, Thornber CR (1987) Geothermometry of Kilauea Iki lava lake, Hawaii. Bull Volcanol 49:651–668

Hofmann DJ (1987) Perturbations to the global atmosphere associated with the El Chichón volcanic eruption of 1982. Rev Geophys 25:743–759

Ishikawa K, Kanisawa S, Aoki K (1980) Content and behavior of fluorine in Japanese Quaternary volcanic rocks and petrogenetic application. J Volcanol Geotherm Res 8:161–175

Iwasaki B, Katsura T (1967) An experimental study of the vaporization of chlorine compounds from basaltic lavas during the cooling process. Bull Chem Soc Jpn 40:1167–1170

Johnson MC, Anderson AT, Rutherford MJ (1994), Pre-eruptive volatile contents of magmas. Rev Mineral 30:281–323

McCormick MP, Thomason LW, Trepte CP (1995) Atmospheric impact of the Mt. Pinatubo eruption. Nature 373:399–404

Mathez EA (1976) Sulfur solubility and magmatic sulfides in submarine basalt glass. J Geophys Res 81:4269–4276

Metrich N (1990) Chlorine and fluorine in tholeiitic and alkaline lavas of Etna (Sicily). J Volcanol Geotherm Res 40:133–148

Metrich N, Clocchiatti R (1989) Melt inclusion investigation of the volatile behavior in historic alkali basaltic magmas of Etna. Bull Volcanol 51:185–198

Metrich N, Sigurdsson H, Meyers PS, Devine JD (1991) The 1783 Lakagígar eruption in Iceland, geochemistry, $CO_2$ and sulfur degassing. Contrib Mineral Petrol 107:435–447

Michael PJ, Schilling J-G (1989) Chlorine in mid-ocean ridge magmas: evidence for assimilation of seawater-influenced components. Geochim Cosmochim Acta 53:3131–3143

Nye CJ, Swanson SE, Avery VF, Miller TP (1994) Geochemistry of the 1989–1990 eruption of Redoubt volcano. Part I. Whole-rock major and trace-element chemistry. J Volcanol Geotherm Res 62:429–452

Ólafsson M, Imsland P, Larsen G (1984) Pele's hair II. Mode of formation, composition and structure. Náttúrufrædingurinn 53:135–144

Óskarsson N, Grönvold K, Larsen G (1984) The haze produced by the Laki eruption. In Einarsson T, Gudbergsson GM, Gunnlaugsson GA, Rafnsson S, Thorarinsson S (eds) Skaftáreldar 1783–1784:Ritgerdir og Heimildir. Mál og Menning, Reykjavík, pp 67–80

Robinson BW, Graham J (1992) Advances in electron microprobe trace-element analysis. J Comput Assist Microscopy 4:263–265

Rose WI (1977) Scavenging of volcanic aerosols by ash: atmospheric and volcanologic implications. Geology 5:621–624

Rowe EC, Schilling J-G (1979) Fluorine in Iceland and Reykjanes ridge basalts. Nature 279:33–37

Self S, Rampino MR, Barbera JJ (1981) The possible effects of large 19th and 20th Century volcanic eruptions on zonal and hemispheric surface temperatures. J Volcanol Geotherm Res 11:41–60

Sigmarsson O, Grönvold K, Condomines M, Thordarson Th (1991) Extreme magma homogeneity in the Lakagígar (Laki) eruption 1783–1784, Iceland. Geophys Res Lett 18:2229–2232

Sigurdsson H (1982) Volcanic pollution and climate: the 1783 Laki eruption. EOS 63:601–602

Sigvaldason GE, Óskarsson N (1976) Chlorine in basalts from Iceland. Geochim Cosmochim Acta 40:777–789

Sigvaldason GE, Óskarsson N (1986) Fluorine in basalts from Iceland. Contrib Mineral Petrol 94:263–271

Shimozuru D (1994) Physical parameters governing the formation of Pele's hair and tears. Bull Volcanol 56:217–219

Steingrímsson J (1783) A short compendium of the recent volcanic outburst in western part of Skaftafell county, dated at Prestbakki July 4, 1783. In: Einarsson T, Gudbergsson GM, Gunnlaugsson GA, Rafnsson S, Thorarinsson S (eds) Skaftáreldar 1783–1784:Ritgerdir og Heimildir. Mál og Menning, Reykjavík, 1984, pp 272–274

Steingrímsson J (1788) A complete description on the Sída volcanic fire, dated November 24, 1788 at Prestbakki. In Safn til Sögu Islands IV, Copenhagen 1907-1915 pp 1–57

Stothers RB (1996) The great dry fog of 1783. Clim Change 32:79–89

Thomason LW, Osborn MT (1992) Lidar conversion parameters derived from Sage II extinction measurements. Geophys Res Lett 19:1655–1658

Thorarinsson S (1979) On the damage caused by volcanic eruptions with special reference to tephra and gases. In: Sheets PD, Grayson DK (eds) Volcanic activity and human geology. Academic Press, New York, pp 125–159

Thorarinsson S (1981) Greetings from Iceland: ash-falls and volcanic aerosols in Scandinavia. Geogr Ann 63:109–118

Thorarinsson S (1984) Pele's hair I. Historical account. Náttúrufrædingurinn 53:127–134

Thordarson Th (1990) The eruption sequence and eruption behavior of the Laki, 1783–1785, Iceland: characteristics and distribution of eruption products. MS thesis, University of Texas at Arlington

Thordarson Th (1991) The Laki 1783–1785, the tephra production and course of events. Special Publication F90018, University of Iceland, 187 pp

Thordarson Th (1995) Volatile release and atmospheric effects of basaltic fissure eruptions. PhD dissertation, University of Hawaii, Honolulu, 570 pp

Thordarson Th, Self S (1990) The Laki lava flow, 1783–1784: new estimates of the volume, flow rates, and flow characteristics. IAVCEI, General Assembly. Mainz, 3–8 September 1990 (abstracts)

Thordarson Th, Self S (1993) The Laki (Skaftár Fires) and Grímsvötn eruptions in 1783–1785. Bull Volcanol 55:233–263

Unni CK, Schilling J-G (1978) Cl and Br degassing by volcanism along the Reykjanes ridge and Iceland. Nature 272:19–23

Vergniolle S, Jaupart C (1986) Separated two-phase flow and basaltic eruptions. J Geophys Res 91:12842–12860

Wallace P, Carmichael ISE (1992) Sulfur in basaltic magmas. Geochim Cosmochim Acta 65:1863–1874

Wallace P, Gerlach TM (1994) Magmatic vapor source for sulfur dioxide released during volcanic eruptions: evidence from Mount Pinatubo. Science 265:497–499

Wilson L, Head JW (1981) Ascent and eruption of basaltic magma on the earth and the moon. J Geophys Res 86:2971–3001

Wood CA (1992) Climatic effects of the 1783 Laki eruption. In: Harrington CR (ed) The year without a summer? Canadian Museum of Nature, Ottawa, pp 58–77

Woods AW (1993) A model of the plumes above basaltic fissure eruptions. Geophys Res Lett 20:1115–1118